Twisting spins and twisting layers

Leon Balents, KITP

College de France, June 10, 2022

Outline

- Twisting spins in Mn_3Sn with a magnetic field
  - Multiple energy scales enable control of anomalous Hall effect

Kamran Behnia
ESPCI

Zengwei Zhu
Wuhan

Xiaokang Li
Wuhan

- Twisting layers of spins in 2d materials
  - Twists control new spin textures

Kasra Hejazi
Caltech

Zhu-Xi Luo
UCSB

Magnets

~500BC: Ferromagnetism documented in Greece, India, used in China

sinan, ~200BC

and in elementary school today

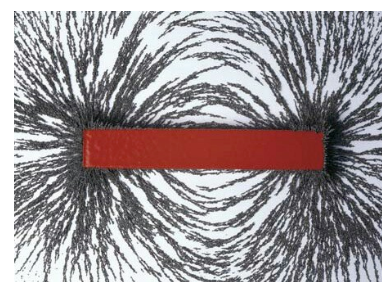

PROPRIÉTÉS MAGNÉTIQUES DES CORPS A DIVERSES TEMPÉRATURES.

Annales de Chimie et de Physique, 7ᵉ série, t. V, 1895, p. 289.

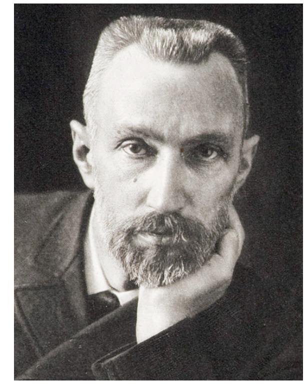

Pierre Curie

Fig. 3.

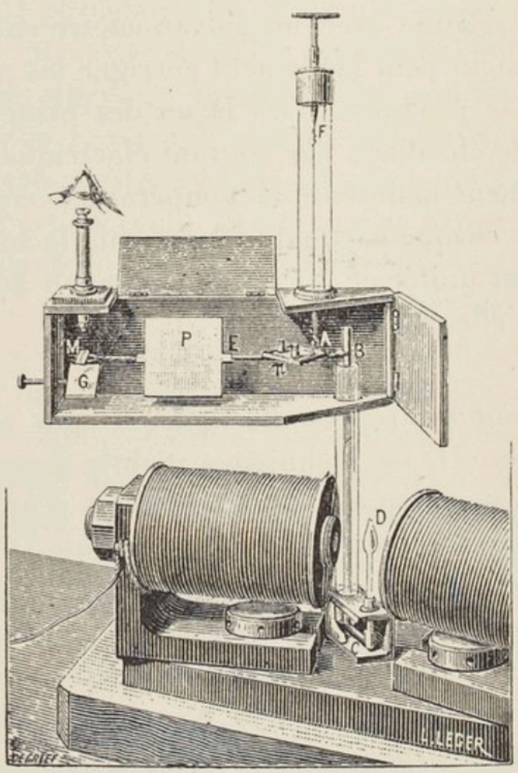

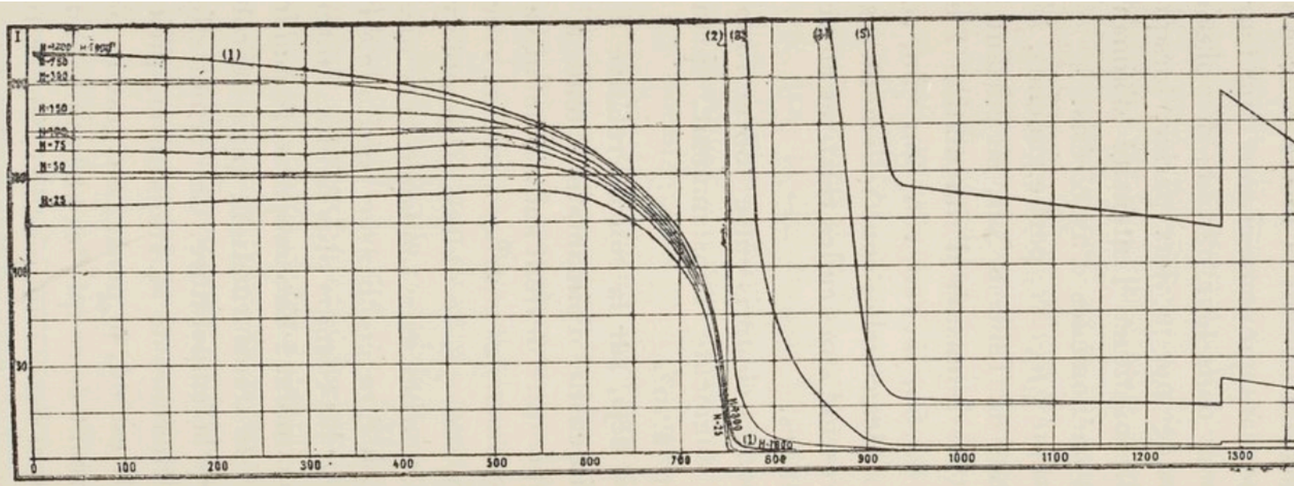

ÉLÉMENTS

DE PHYSIQUE

EXPÉRIMENTALE

ET DE MÉTÉOROLOGIE

PAR

M. POUILLET

MEMBRE DE L'INSTITUT (ACADÉMIE DES SCIENCES)

203. **Influence de la chaleur sur le magnétisme.** — Nous avons déjà dit qu'un aimant artificiel ou naturel, chauffé jusqu'au rouge blanc, perd complétement son magnétisme, de telle sorte qu'il n'est plus, après le refroidissement, qu'un corps inerte, sans force directrice et sans force magnétique. Cette observation est fort ancienne; elle avait été faite par Gilbert.

Quelques analogies assez remarquables entre les distances des atomes des corps et leurs propriétés magnétiques m'avaient conduit à penser que la limite magnétique des différents corps devait se trouver à des températures très-différentes, et j'ai, en effet, démontré par l'expérience :

1° Que le cobalt ne cesse jamais d'être magnétique, ou plutôt que sa limite magnétique est à une température plus haute que le rouge blanc le plus éclatant;

2° Que le chrome a sa limite magnétique un peu au-dessus de la température rouge sombre;

3° Que le nickel a sa limite magnétique vers 350°, à peu près à la température de la fusion du zinc;

4° Enfin, que le manganèse a sa limite magnétique à la température de 20 à 25° au-dessus de 0°.

ÉLÉMENTS

DE PHYSIQUE

EXPÉRIMENTALE

ET DE MÉTÉOROLOGIE

PAR

M. POUILLET

MEMBRE DE L'INSTITUT (ACADÉMIE DES SCIENCES)

203. Influence de la chaleur sur le magnétisme. — Nous avons déjà dit qu'un aimant artificiel ou naturel, chauffé jusqu'au rouge blanc, perd complétement son magnétisme, de telle sorte qu'il n'est plus, après le refroidissement, qu'un corps inerte, sans force directrice et sans force magnétique. Cette observation est fort ancienne; elle avait été faite par Gilbert.

Quelques analogies assez remarquables entre les distances des atomes des corps et leurs propriétés magnétiques m'avaient conduit à penser que la limite magnétique des différents corps devait se trouver à des températures très-différentes, et j'ai, en effet, démontré par l'expérience :

1° Que le cobalt ne cesse jamais d'être magnétique, ou plutôt que sa limite magnétique est à une température plus haute que le rouge blanc le plus éclatant;

2° Que le chrome a sa limite magnétique un peu au-dessus de la température rouge sombre;

3° Que le nickel a sa limite magnétique vers 350°, à peu près à la température de la fusion du zinc;

4° Enfin, que le manganèse a sa limite magnétique à la température de 20 à 25° au-dessus de 0°.

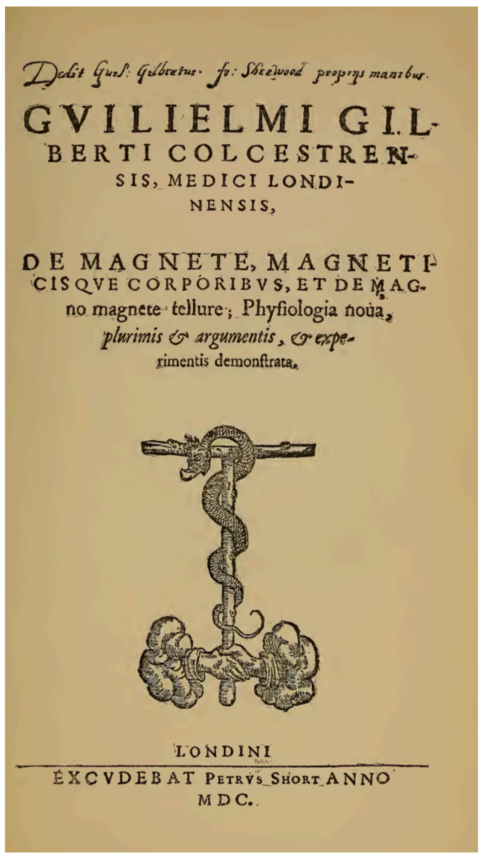

Dedit Guil: Gilbertus· Fr: Sherwood proprijs manibus.

GVILIELMI GILBERTI COLCESTRENSIS, MEDICI LONDINENSIS,

DE MAGNETE, MAGNETICISQVE CORPORIBVS, ET DE MAGno magnete tellure; Physiologia noua, *plurimis & argumentis, & experimentis demonstrata.*

LONDINI

EXCVDEBAT PETRVS SHORT ANNO MDC.

Magnetism

- Atomic spins interact via *exchange* to favor an ordered arrangement

  - Aligned parallel: ferromagnets

$$H = -J \sum_{\langle ij \rangle} \boldsymbol{S}_i \cdot \boldsymbol{S}_j$$

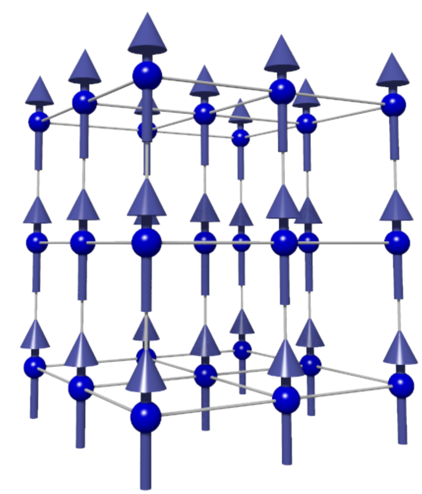

Magnetism

- Atomic spins interact via *exchange* to favor an ordered arrangement
  - More complex arrangements: antiferromagnets

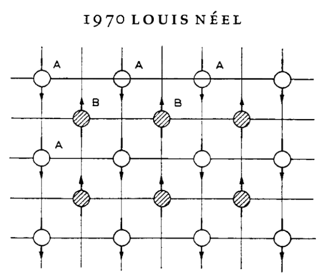

Louis Néel

1949AD: antiferromagnetism proven experimentally

but there are 1000s of them, much more common than FMs

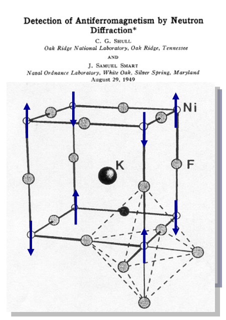
Detection of Antiferromagnetism by Neutron Diffraction*
C. G. Shull
Oak Ridge National Laboratory, Oak Ridge, Tennessee
and
J. Samuel Smart
Naval Ordnance Laboratory, White Oak, Silver Spring, Maryland
August 29, 1949

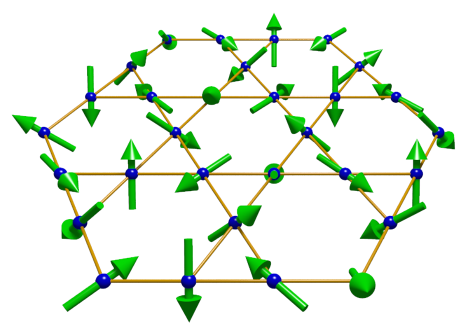

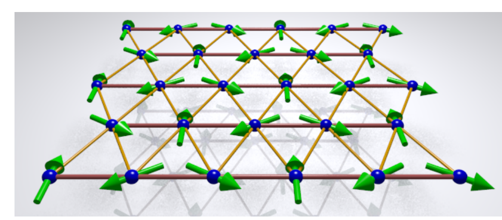

AHE

"Anomalous" Hall effect: a field-independent contribution to the Hall effect due to magnetic order

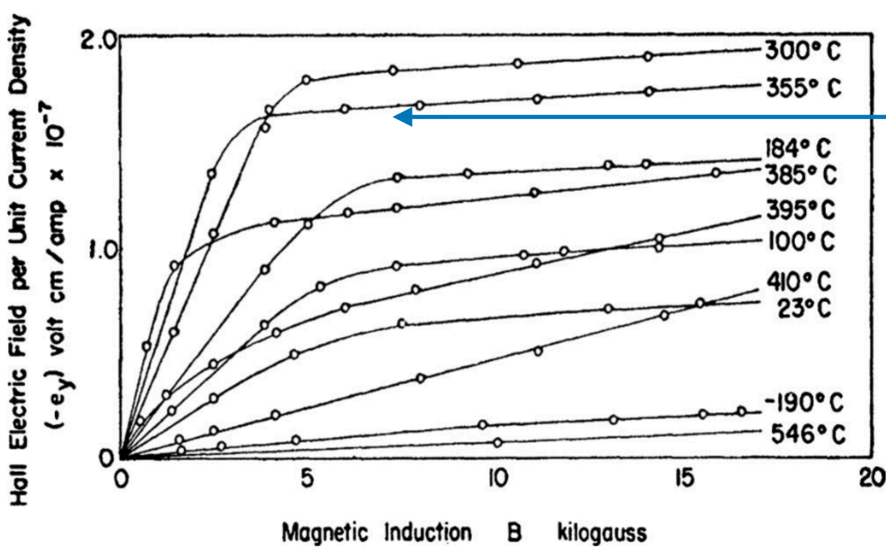

FIG. 1. The Hall effect in Ni (data from Smith, 1910). From Pugh and Rostoker, 1953.

$$\rho_H = R_H B + \rho_{AH}$$

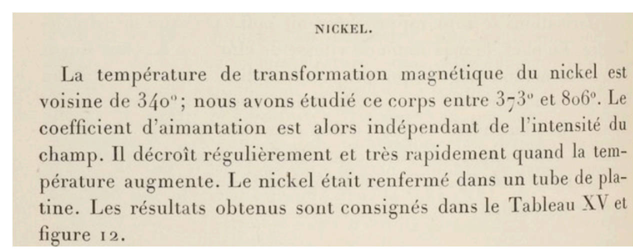
NICKEL.

La température de transformation magnétique du nickel est voisine de 340°; nous avons étudié ce corps entre 373° et 806°. Le coefficient d'aimantation est alors indépendant de l'intensité du champ. Il décroît régulièrement et très rapidement quand la température augmente. Le nickel était renfermé dans un tube de platine. Les résultats obtenus sont consignés dans le Tableau XV et figure 12.

Commonly seen in ferromagnets

Mn_3Sn

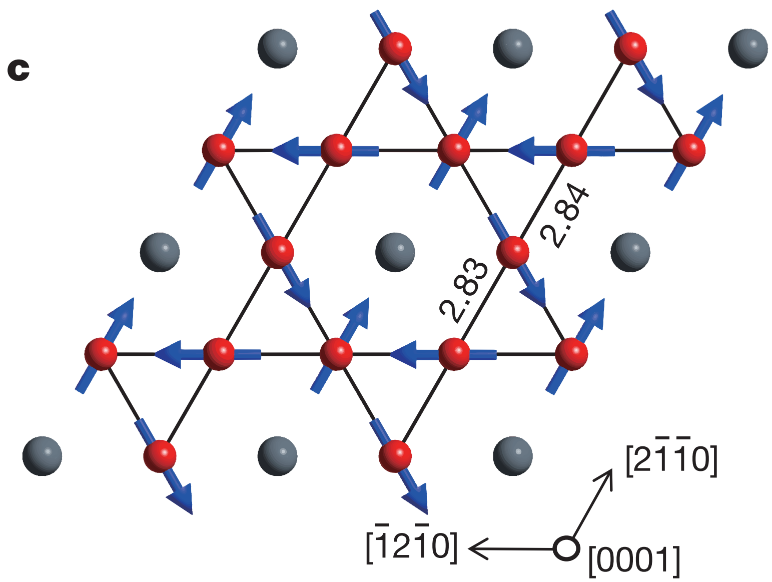

Spins arranged into elementary triangles - "kagomé"

large ordered *antiferromagnetic* moment

~ 2 μ_B /Mn

tiny FM moment:

.002 μ_B/Mn

T_N ~ 420K

Nagamiya *et al*, 1982

AHE

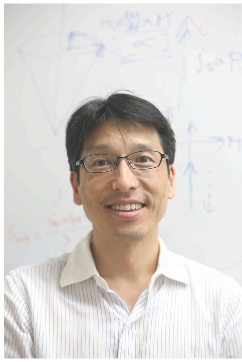

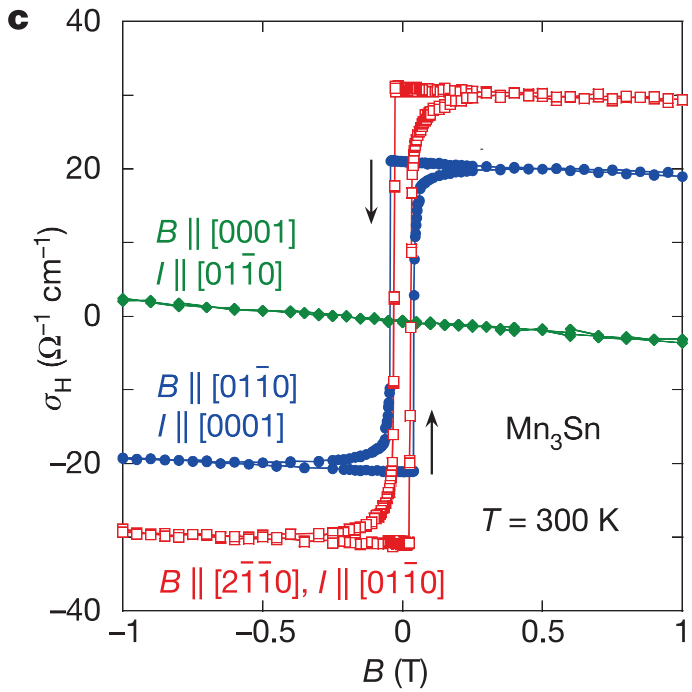

S. Nakatsuji *et al*, 2015

<u>Mn_3Sn:</u>

Large "anomalous" Hall conductivity

Tiny magnetization

Small coercive field

These properties are a desirable combination

Anomalous Nernst Effect

Related effect with potential thermoelectric applications

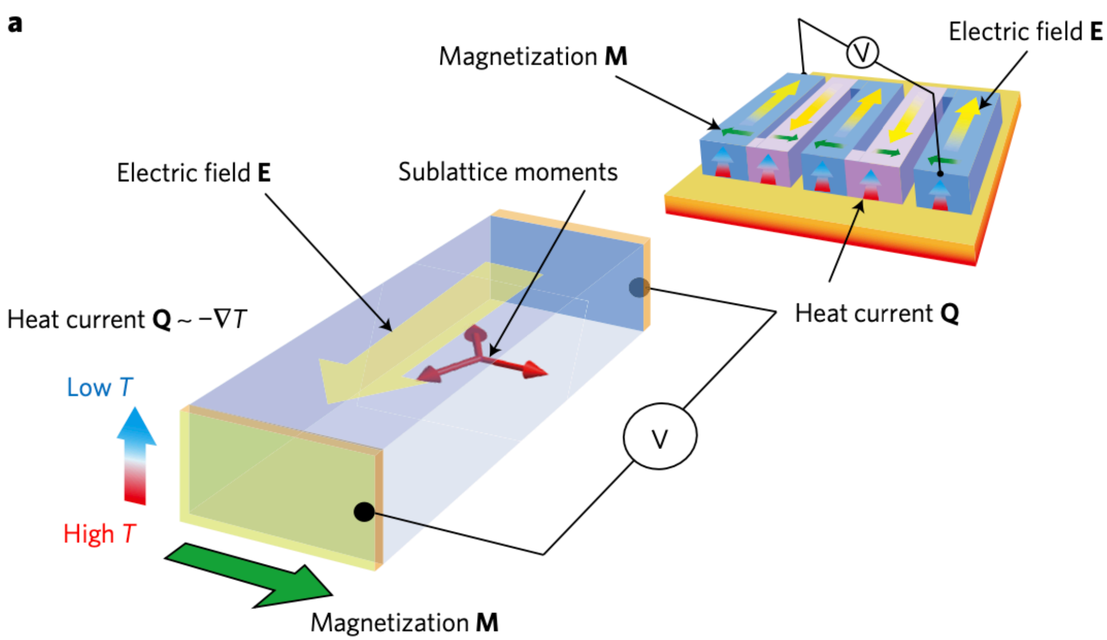

Electric field perpendicular to temperature gradient

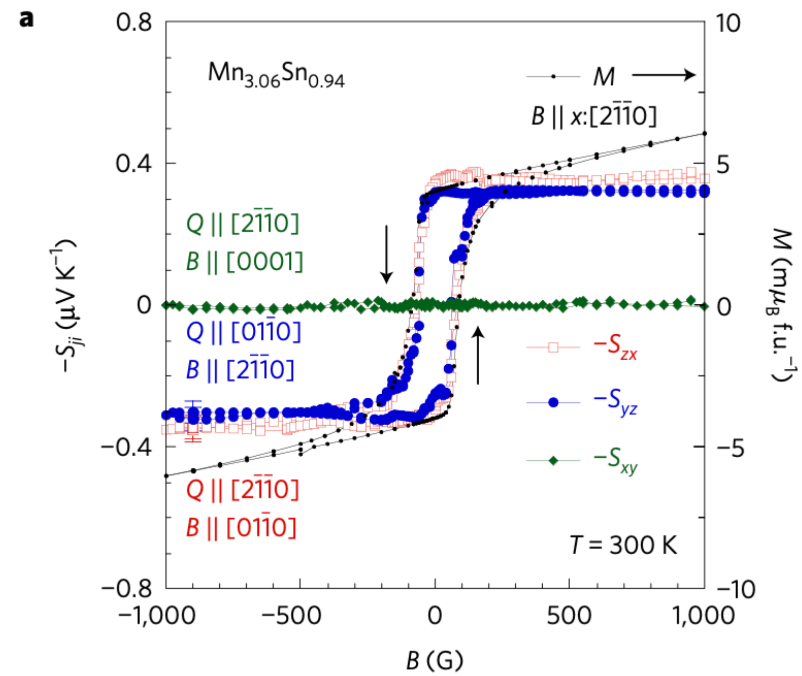

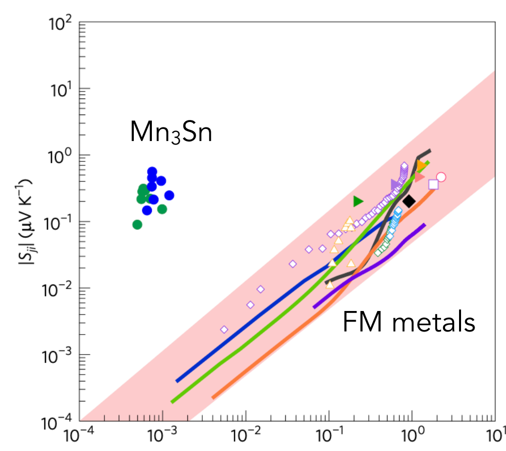

AHE

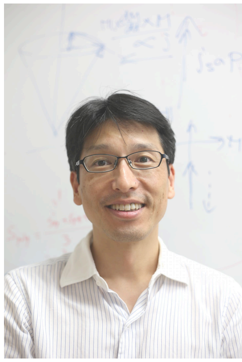

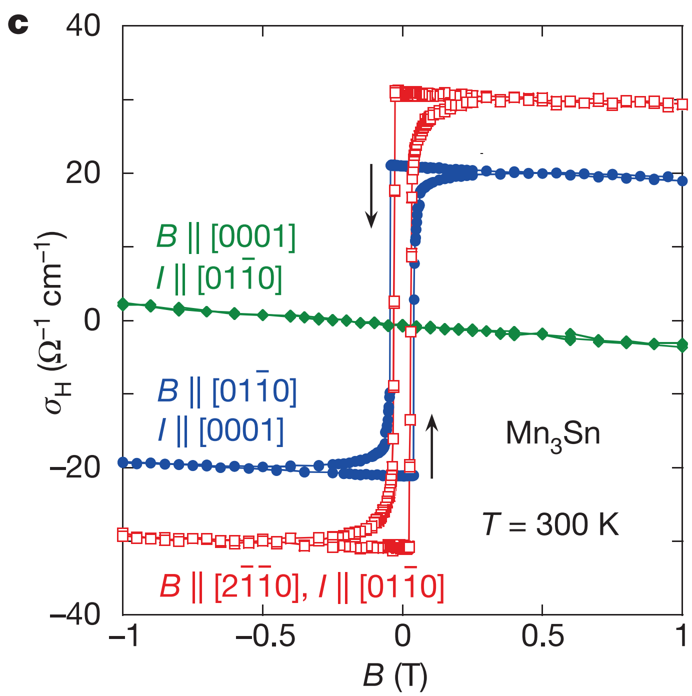

S. Nakatsuji *et al*, 2015

<u>Mn_3Sn:</u>

Large "anomalous" Hall conductivity

Tiny magnetization

Small coercive field

How do these properties go together???

Twisting wave functions

Intrinsic anomalous Hall effect from Berry curvature:

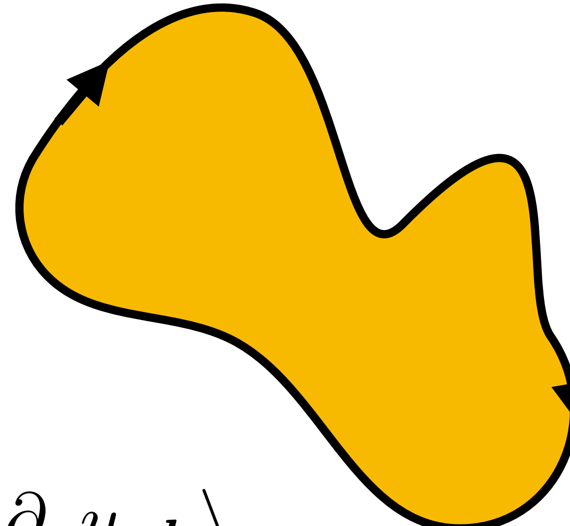

$$\sigma_{\mu\nu}^{\mathrm{AH}} = \frac{e^2}{\hbar}\epsilon_{\mu\nu\lambda}\Omega_\lambda$$

$$\Omega_\lambda = \epsilon_{\mu\nu\lambda}\sum_n \int \frac{d^3\boldsymbol{k}}{(2\pi)^3}\, n_F(\epsilon_{n\boldsymbol{k}})\, \langle \partial_\mu u_{n\boldsymbol{k}} | \partial_\nu u_{n\boldsymbol{k}} \rangle$$

Karplus+Luttinger, 1954

<u>Physical meaning:</u>

"Flux" of Berry curvature gives phase accumulated in an electron's orbit

Thouless, Haldane

Twisting wave functions

Hall vector ***Ω***: $\sigma^{\mathrm{AH}}_{\mu\nu} = \frac{e^2}{\hbar}\epsilon_{\mu\nu\lambda}\Omega_\lambda$

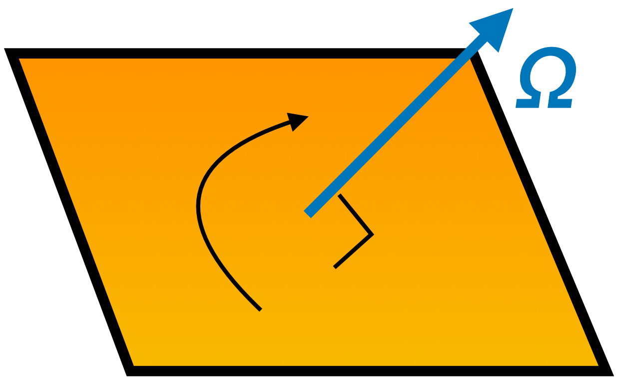

Ω Determines plane of Hall effect

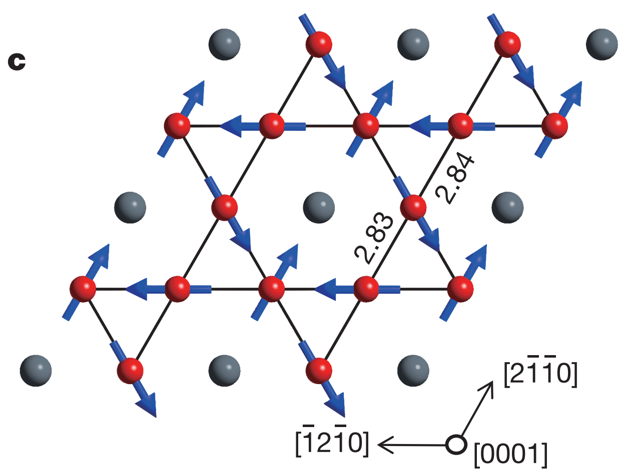

Spin configuration determines ***Ω*** through influence on electrons

Because *local* moments are not small, neither is ***Ω***

AHE

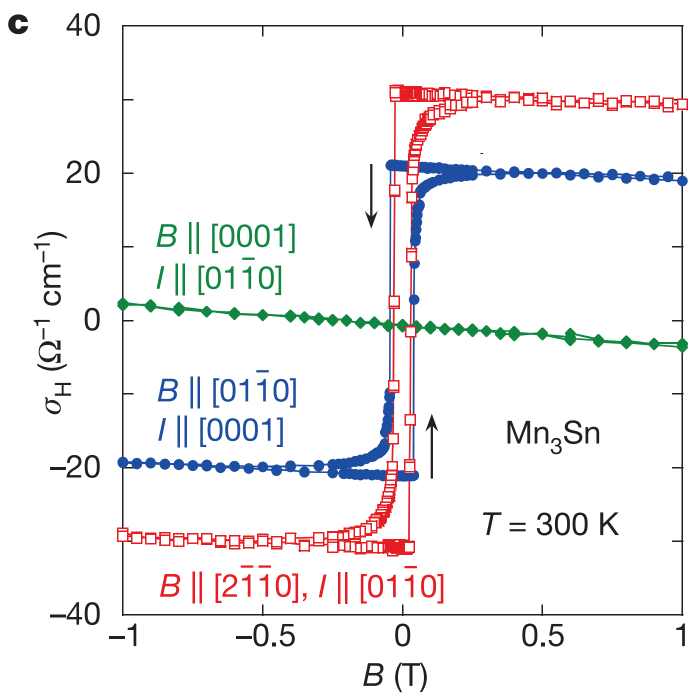

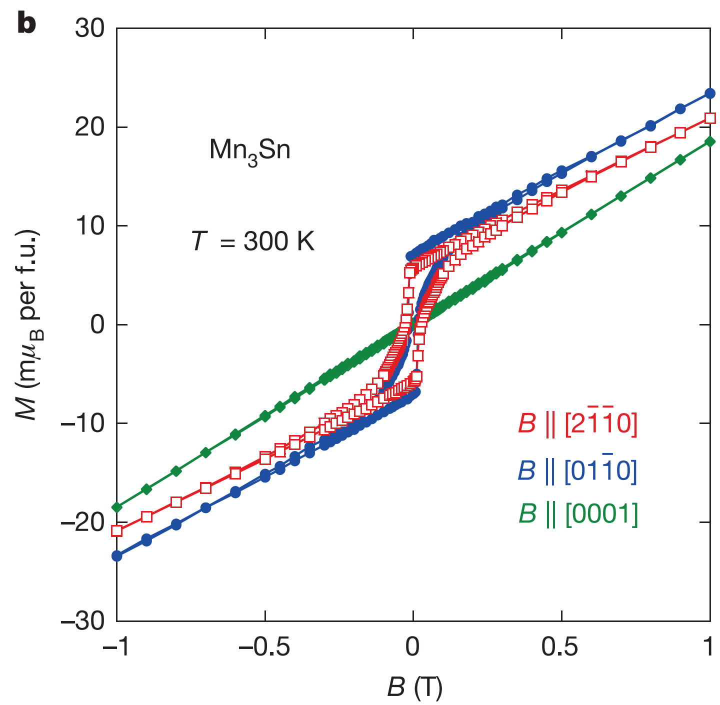

S. Nakatsuji *et al*, 2015

Why such a tiny moment?

Why such small coercive field?

AHE

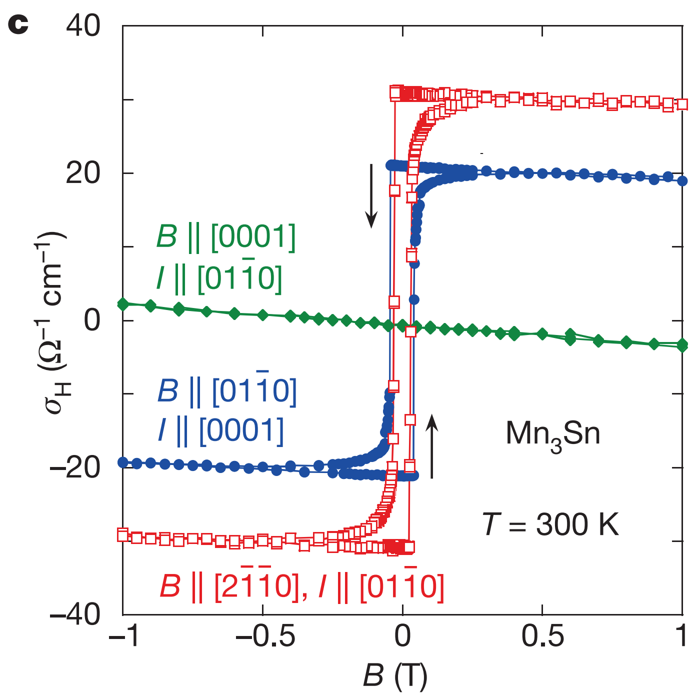

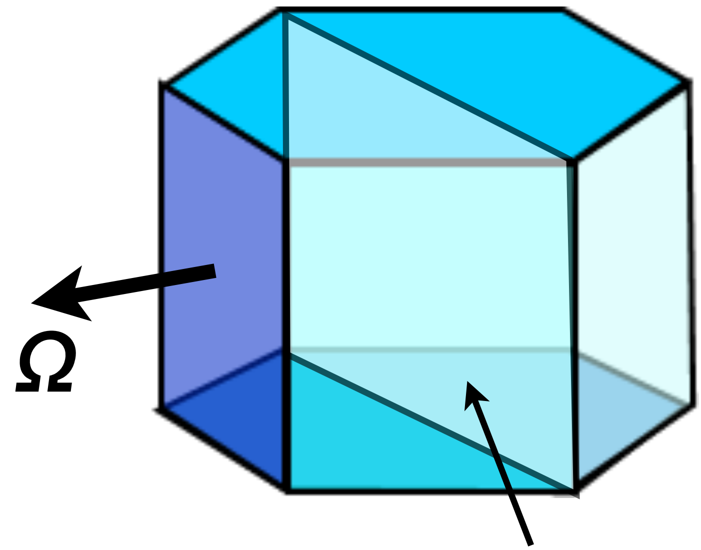

Hall effect in *vertical* plane

Why such a tiny moment?

For B>.2T, plane of the AHE follows the field

Energetics: triangle

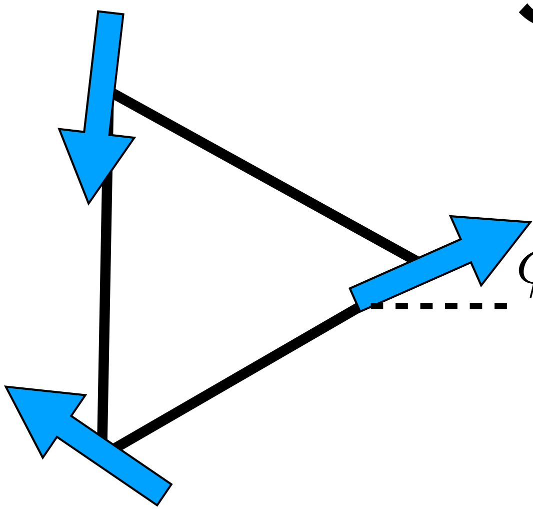

$$E = J\left(\boldsymbol{S}_1 \cdot \boldsymbol{S}_2 + \boldsymbol{S}_2 \cdot \boldsymbol{S}_3 + \boldsymbol{S}_3 \cdot \boldsymbol{S}_1\right)$$
$$+ D\hat{\boldsymbol{z}} \cdot \left(\boldsymbol{S}_1 \times \boldsymbol{S}_2 + \boldsymbol{S}_2 \times \boldsymbol{S}_3 + \boldsymbol{S}_3 \times \boldsymbol{S}_1\right)$$
$$- K \sum_i \left(\hat{n}_i \cdot \boldsymbol{S}_i\right)^2$$

Jianpeng Liu + LB, 2017

$J \gg D \gg K$ **Hierarchy of interactions**

- J: spins at 120° angles and M=0
- D: spins are "anti-chiral" in XY plane
- K: weak canting toward easy axes creates tiny moment, and even tinier preference for ϕ

Energetics: triangle

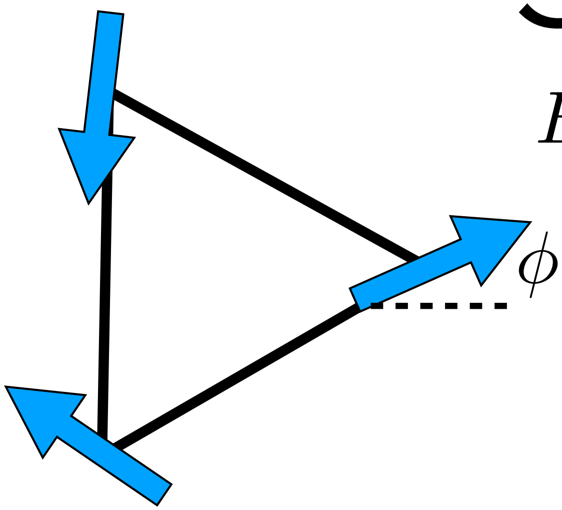

$$E = J\left(\boldsymbol{S}_1 \cdot \boldsymbol{S}_2 + \boldsymbol{S}_2 \cdot \boldsymbol{S}_3 + \boldsymbol{S}_3 \cdot \boldsymbol{S}_1\right)$$

$$+D\hat{\boldsymbol{z}} \cdot \left(\boldsymbol{S}_1 \times \boldsymbol{S}_2 + \boldsymbol{S}_2 \times \boldsymbol{S}_3 + \boldsymbol{S}_3 \times \boldsymbol{S}_1\right)$$

$$-K \sum_i \left(\hat{n}_i \cdot \boldsymbol{S}_i\right)^2$$

Jianpeng Liu + LB, 2017

$J \gg D \gg K$ **Hierarchy of interactions**

- J: spins at 120° angles and M=0
- D: spins are "anti-chiral" in XY plane
- K: weak canting toward easy axes creates tiny moment, and even tinier preference for ϕ

Global symmetries: spin-space group

magnetic space group

Energetics: triangle

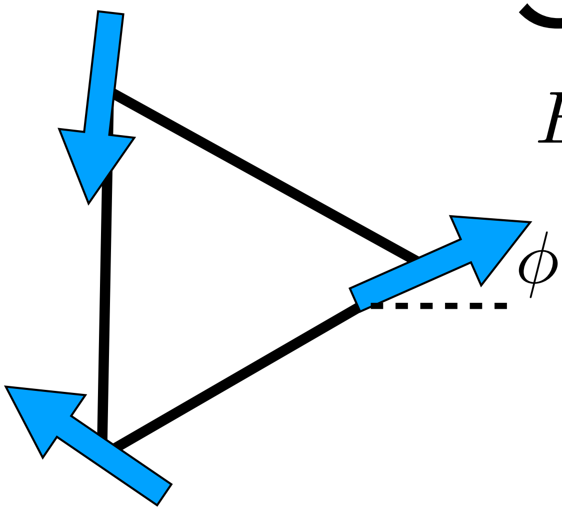

$$E = J\left(\boldsymbol{S}_1 \cdot \boldsymbol{S}_2 + \boldsymbol{S}_2 \cdot \boldsymbol{S}_3 + \boldsymbol{S}_3 \cdot \boldsymbol{S}_1\right)$$

$$+D\hat{\boldsymbol{z}} \cdot \left(\boldsymbol{S}_1 \times \boldsymbol{S}_2 + \boldsymbol{S}_2 \times \boldsymbol{S}_3 + \boldsymbol{S}_3 \times \boldsymbol{S}_1\right)$$

$$-K \sum_i \left(\hat{n}_i \cdot \boldsymbol{S}_i\right)^2$$

Jianpeng Liu + LB, 2017

$J \gg D \gg K$ **Hierarchy of interactions**

$$m_0 = \frac{K}{J} m_s$$ Uniform moment

$$\lambda = \frac{K^3}{12J^2}$$ In-plane anisotropy

Low coercive field despite tiny Zeeman energy

Energetics: triangle

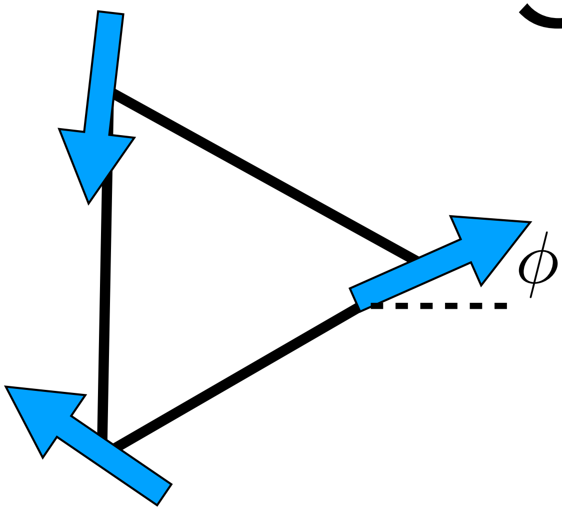

$$\mathbf{\Omega} = |\Omega| \begin{pmatrix} \cos\phi \\ -\sin\phi \\ 0 \end{pmatrix}$$

Jianpeng Liu + LB, 2017

$J \gg D \gg K$ **Hierarchy of interactions**

$$m_0 = \frac{K}{J} m_s$$ Uniform moment

$$\lambda = \frac{K^3}{12J^2}$$ In-plane anisotropy

Low coercive field despite tiny Zeeman energy

Torque

Kamran Behnia
ESPCI

Zengwei Zhu
Wuhan

Xiaokang Li
Wuhan

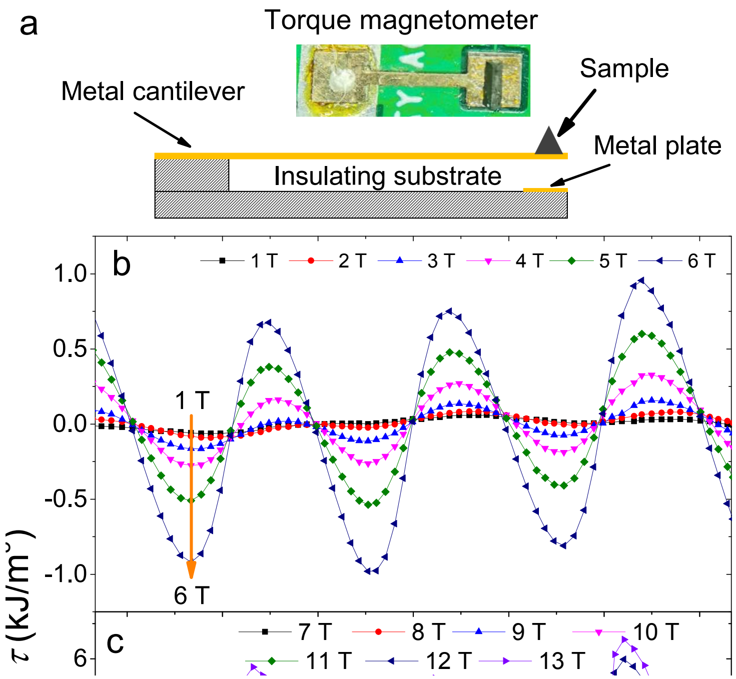

$$\boldsymbol{\tau} = \boldsymbol{M} \times \boldsymbol{B}$$

Tracks *mis*-alignment of ***M*** with ***B***.

Total ***M*** results from twists that spoil cancellation of antiferromagnetically aligned spins.

Torque

Kamran Behnia
ESPCI

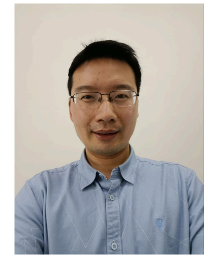

Zengwei Zhu
Wuhan

Xiaokang Li
Wuhan

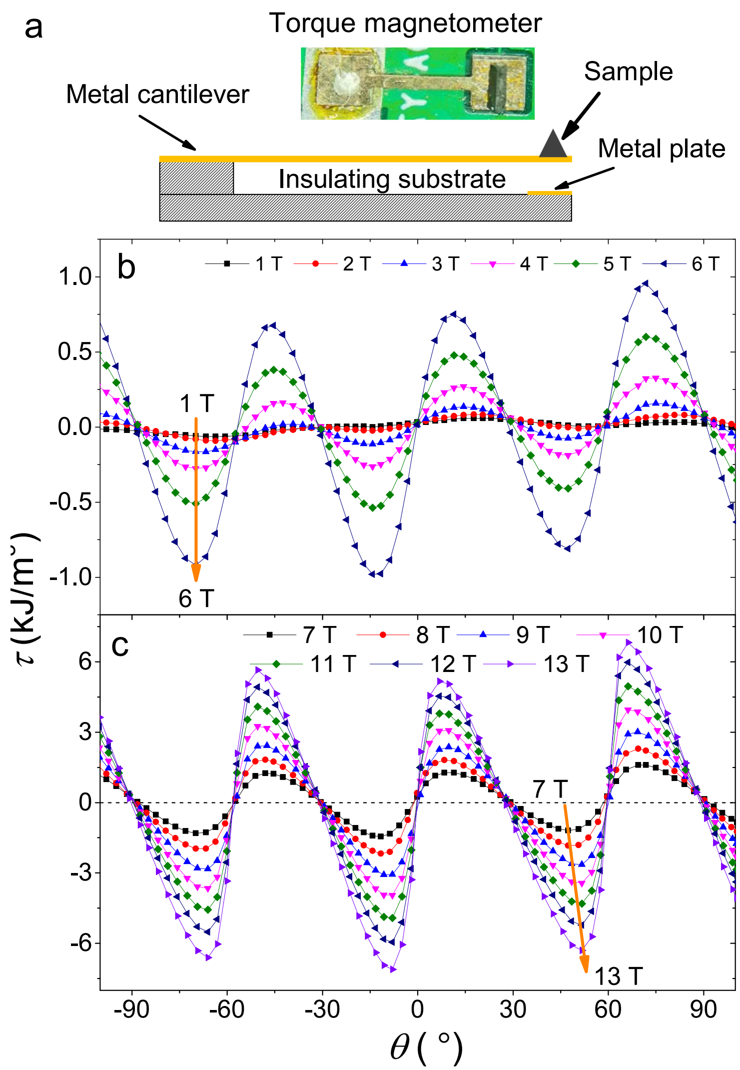

The free energy of twisting spins in Mn_3Sn

Xiaokang Li[1,*], Shan Jiang[3,1], Qingkai Meng[1], Huakun Zuo[1], Zengwei Zhu[1,*], Leon Balents[2,4] and Kamran Behnia[3]

(1) Wuhan National High Magnetic Field Center and School of Physics, Huazhong University of Science and Technology, Wuhan 430074, China

(2)Kavli Institute for Theoretical Physics, University of California, Santa Barbara, California 93106-4030, USA

(3) Laboratoire de Physique et d'Étude des Matériaux (ESPCI - CNRS - Sorbonne Université), PSL Research University, 75005 Paris, France

(4) Canadian Institute for Advanced Research, Toronto, Ontario, Canada

(Dated: February 25, 2022)

Notice the evolution from sinusoidal to sawtooth

First explanation

Extension of our expansion from 2017

$$\phi_1 = \phi + \eta_1, \qquad \phi_2 = \phi - \frac{2\pi}{3} + \eta_2, \qquad \phi_3 = \phi - \frac{4\pi}{3} - \eta_1 - \eta_2.$$

$$\eta_i = \sum_{n=1}^{\infty} \eta_{i,n} r^n, \qquad E_{u.c.} = \sum_{n=0}^{\infty} E_{u.c.}^{(n)},$$

$$\begin{aligned}
E_{u.c.}^{(0)} &= -6J - 6\sqrt{3}D,\\
E_{u.c.}^{(1)} &= -3K,\\
E_{u.c.}^{(2)} &= -\frac{(\mu H)^2 + K^2 + 2\mu H K\cos(\theta+\phi)}{2\left(\sqrt{3}D + J\right)},\\
E_{u.c.}^{(3)} &= -\frac{1}{36(J+\sqrt{3}D)^3}\Big[(3J+7\sqrt{3}D)K^3\cos(6\phi) + 6(J+3\sqrt{3}D)\mu H K^2\cos(5\phi-\theta)\\
&\quad + 3(J+5\sqrt{3}D)(\mu H)^2 K\cos(4\phi-2\theta) + 4\sqrt{3}D(\mu H)^3\cos(3\phi-3\theta)\Big].
\end{aligned}$$

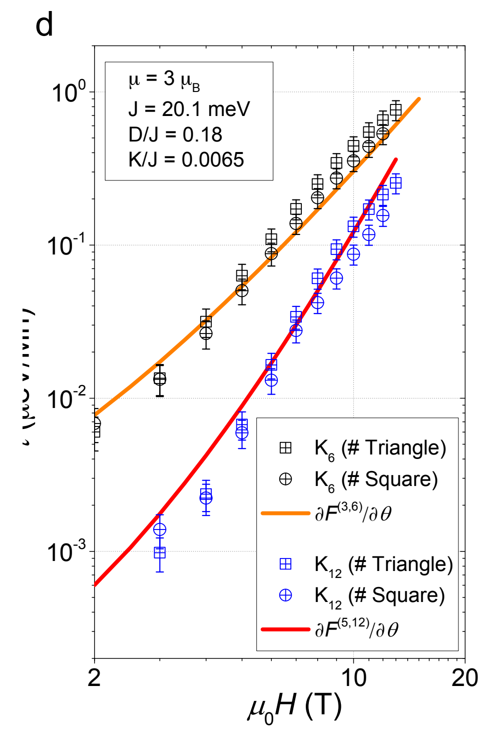

Perturbatively solve $\phi(\theta)$

$$E_{u.c.} = -6J - 6\sqrt{3}D - 3K - \frac{(\mu H + K)^2}{2(J+\sqrt{3}D)}\Big[1 + \frac{(3J+7\sqrt{3}D)K + 4\sqrt{3}D\mu H}{18(J+\sqrt{3}D)^2}\cos(6\theta)$$
$$+ \frac{\left((3J+7\sqrt{3}D)K^2 + 2(J+4\sqrt{3}D)\mu H K + 2\sqrt{3}D(\mu H)^2\right)^2}{36(J+\sqrt{3}D)^4\mu H K}\sin^2(6\theta)\Big].$$

Angular transitions

A little simpler picture

Heisenberg model

$$E_{\text{tri}} = \frac{J}{2}\left(\boldsymbol{S}_1 + \boldsymbol{S}_2 + \boldsymbol{S}_3 - \frac{1}{J}\boldsymbol{h}\right)^2$$

"Order by disorder": thermal and quantum fluctuations favor coplanar states

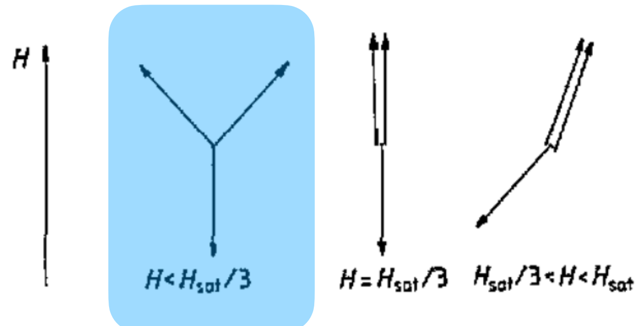

Figure 1. Reorientation process in the magnetic field in 2D Heisenberg AFM on a triangular lattice. Zero-point fluctuations stabilize the collinear phase in the finite region $H_1 < H < H_2$ in the vicinity of $H_{sat}/3$.

A. Chubukov and I. Golosov, 1991

Experiments

PHYSICAL REVIEW B **92**, 014414 (2015)

Magnetic phase diagram of $Ba_3CoSb_2O_9$ as determined by ultrasound velocity measurements

G. Quirion,* M. Lapointe-Major, M. Poirier, and J. A. Quilliam
Département de Physique, Université de Sherbrooke, Sherbrooke, Québec, Canada J1K 2R1

Z. L. Dun and H. D. Zhou
Department of Physics and Astronomy, University of Tennessee, Knoxville, Tennessee, 37996-1200, USA
(Received 8 April 2015; revised manuscript received 26 May 2015; published 13 July 2015)

Numerous examples amongst insulating anti-ferromagnets

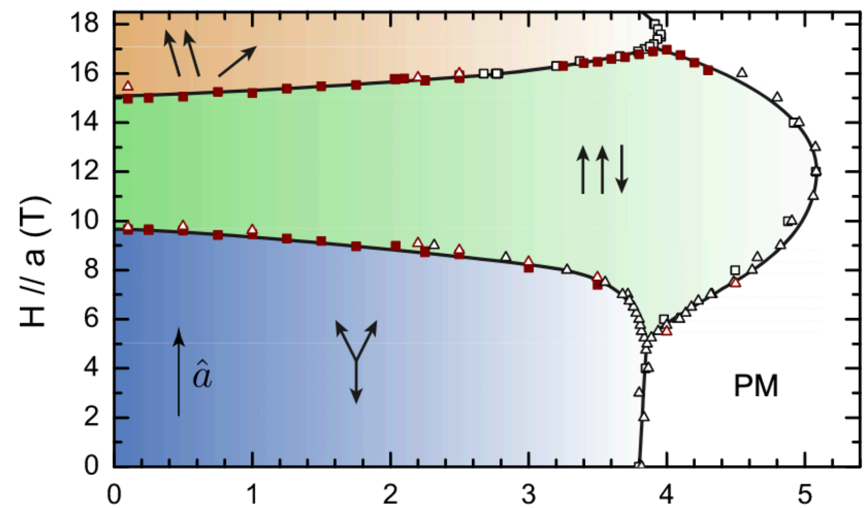

c.f.

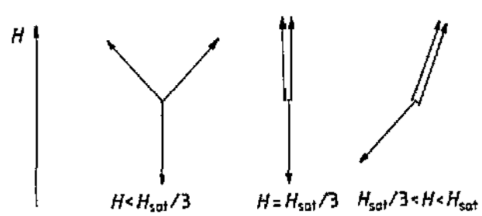

Figure 1. Reorientation process in the magnetic field in 2D Heisenberg AFM on a triangular lattice. Zero-point fluctuations stabilize the collinear phase in the finite region $H_1 < H < H_2$ in the vicinity of $H_{sat}/3$.

Energy and symmetries: Heisenberg limit

$$\langle \boldsymbol{S}_n \rangle = \mathrm{Re}\left[\boldsymbol{d}\, e^{\frac{2\pi i n}{3}}\right]$$

$$\boldsymbol{d}\cdot\boldsymbol{d} = 0.$$

$$\boldsymbol{d} = \boldsymbol{u} + i\boldsymbol{v}$$

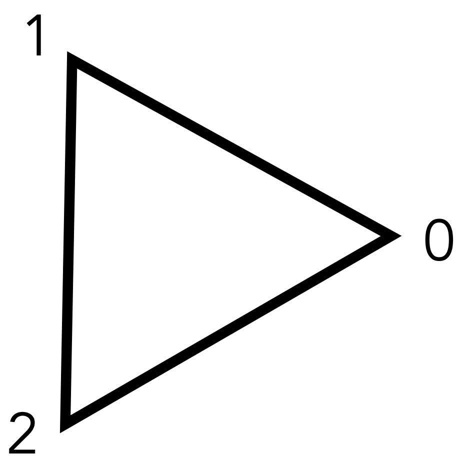

SO(3) $\boldsymbol{S}_n \rightarrow \mathsf{O}\boldsymbol{S}_n$

S_3 $\boldsymbol{S}_n \rightarrow \boldsymbol{S}_{P(n)}$

$$F_h^{\mathrm{iso}} = c_1|\boldsymbol{h}\cdot\boldsymbol{d}|^2 + c_2\mathrm{Re}\left[(\boldsymbol{h}\cdot\boldsymbol{d})^3\right] + O(h^4)$$

Selects plane — Selects angle in plane

$c_1 < 0$ — $c_2 > 0$

Coefficients are “large”: arise from J >> D,K

Quadratic magnetization

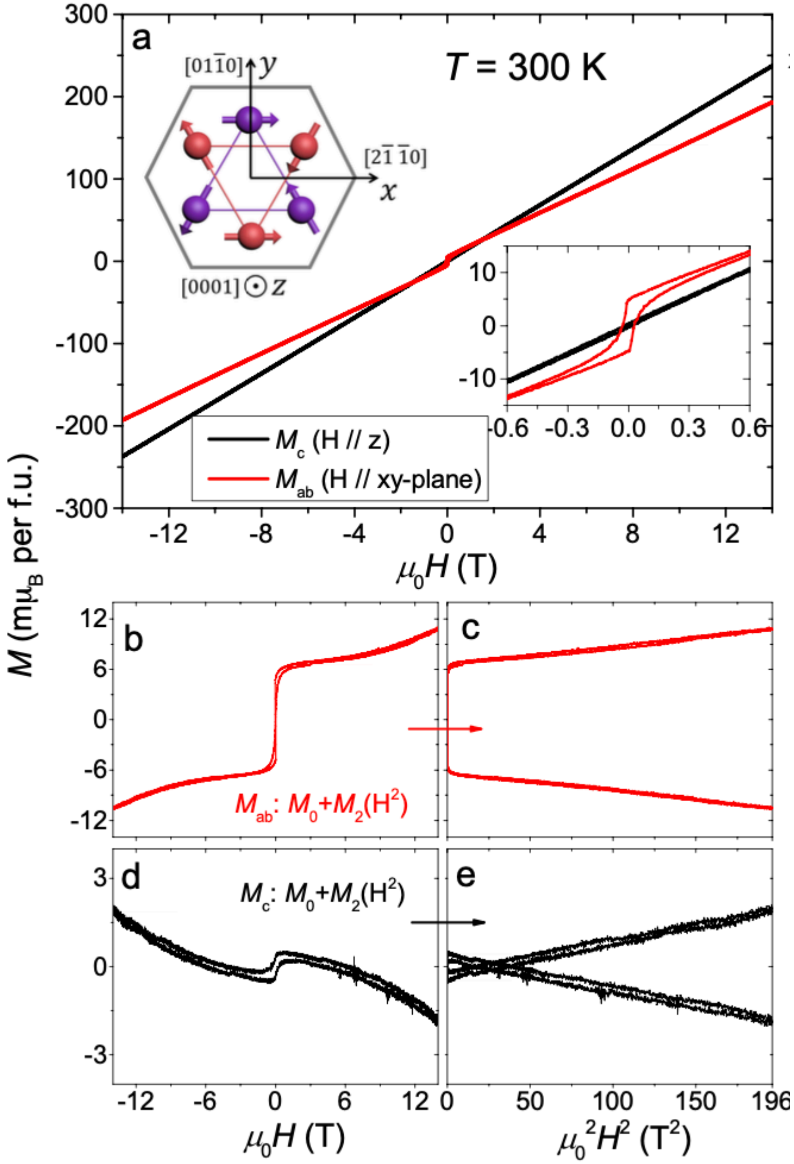

Thermodynamics:

$$M = -\frac{\partial F}{\partial H}$$

$$\sim c_1 H + c_2 H^2$$

Can directly see the energy responsible for order by disorder !

Anti-chiral state

Favored by D>0 $\boldsymbol{d} = d e^{i\phi} \left(\hat{\boldsymbol{x}} + i \hat{\boldsymbol{y}} \right)$

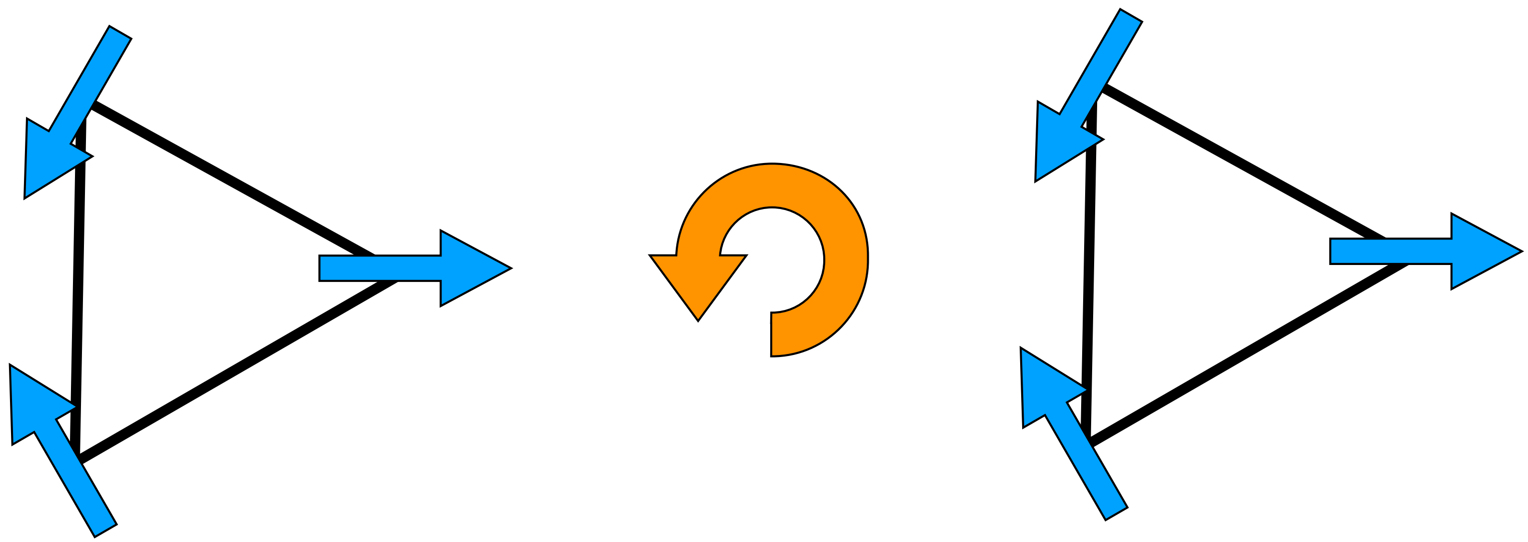

counter-clockwise rigid rotation = clockwise spin rotation

$d_\pm = d_x \pm i d_y \quad h_\pm = h_x \pm i h_y$

Re[h_+ d_+] is an invariant

Full angular free energy

$$d_+ = ne^{i\phi}$$

$$d_- = d_z = 0$$

$$h_+ = he^{i\theta}$$

Zero field anisotropy
(Negligible)

$$f_+ = -w\cos 6\phi - uh\cos(\phi+\theta) - vh^3\cos 3(\phi-\theta)$$

Anti-chiral magnetization

Heisenberg response

$$u \sim \frac{K}{J}$$

Full angular free energy

$$d_+ = ne^{i\phi}$$
$$d_- = d_z = 0$$

$$h_+ = he^{i\theta}$$

$$f_+ = \quad -uh\cos(\phi+\theta) - vh^3\cos 3(\phi-\theta)$$

Anti-chiral magnetization

Heisenberg response

small h:

$$\phi \approx -\theta$$

large h:

$$\phi \approx \theta + \frac{2\pi k}{3}$$

Angular evolution

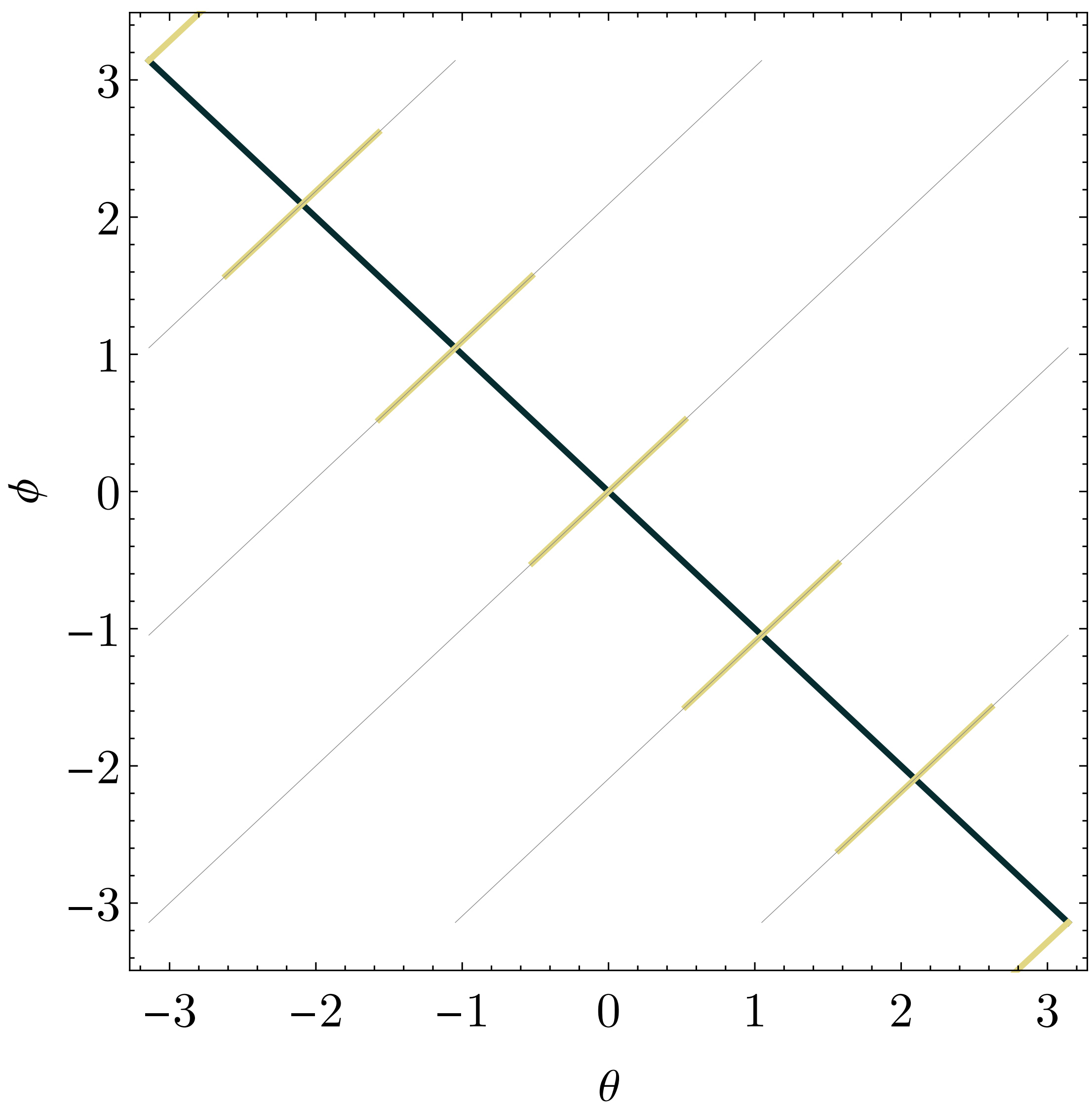

Angular evolution

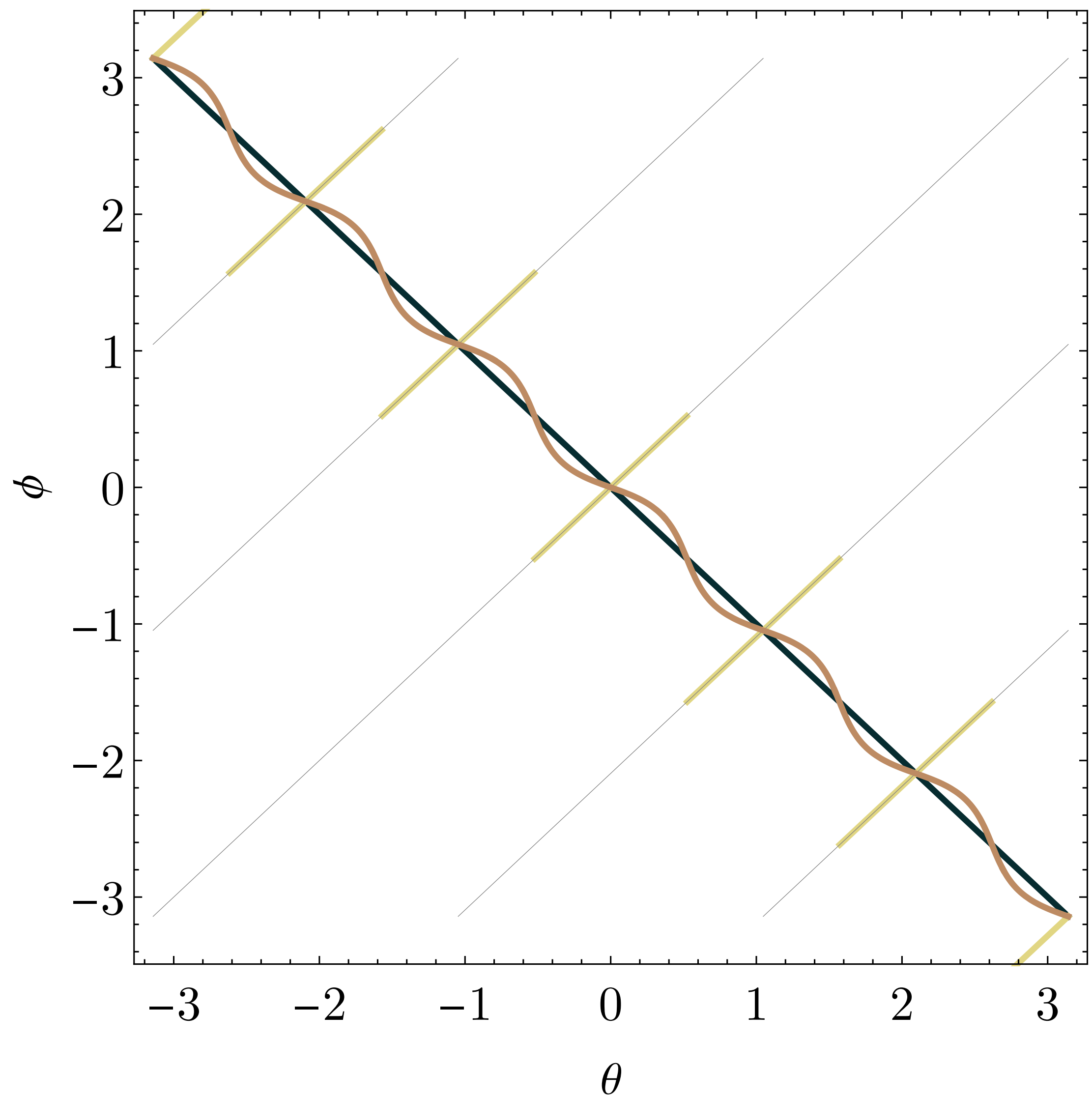

Angular evolution

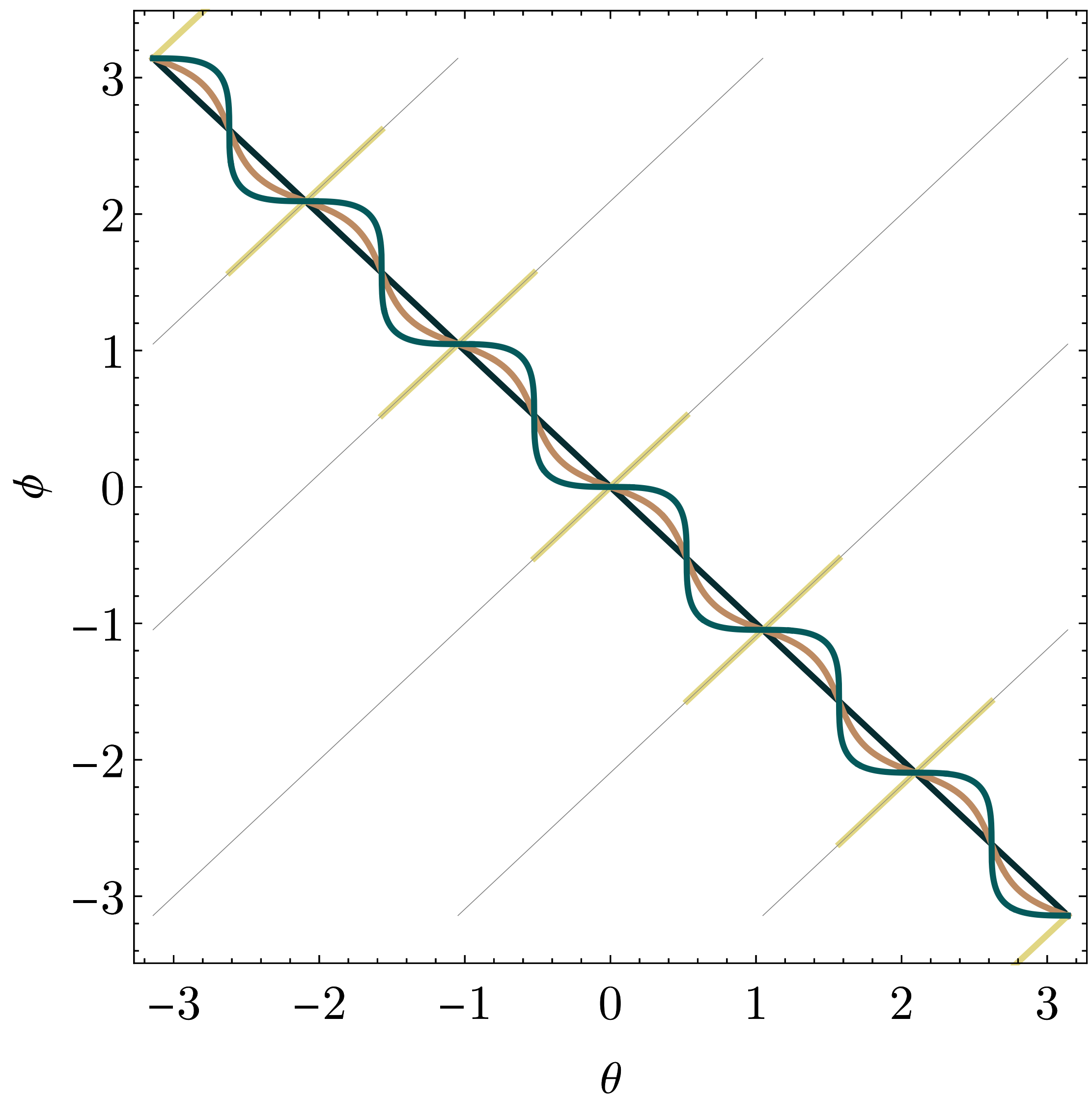

Angular evolution

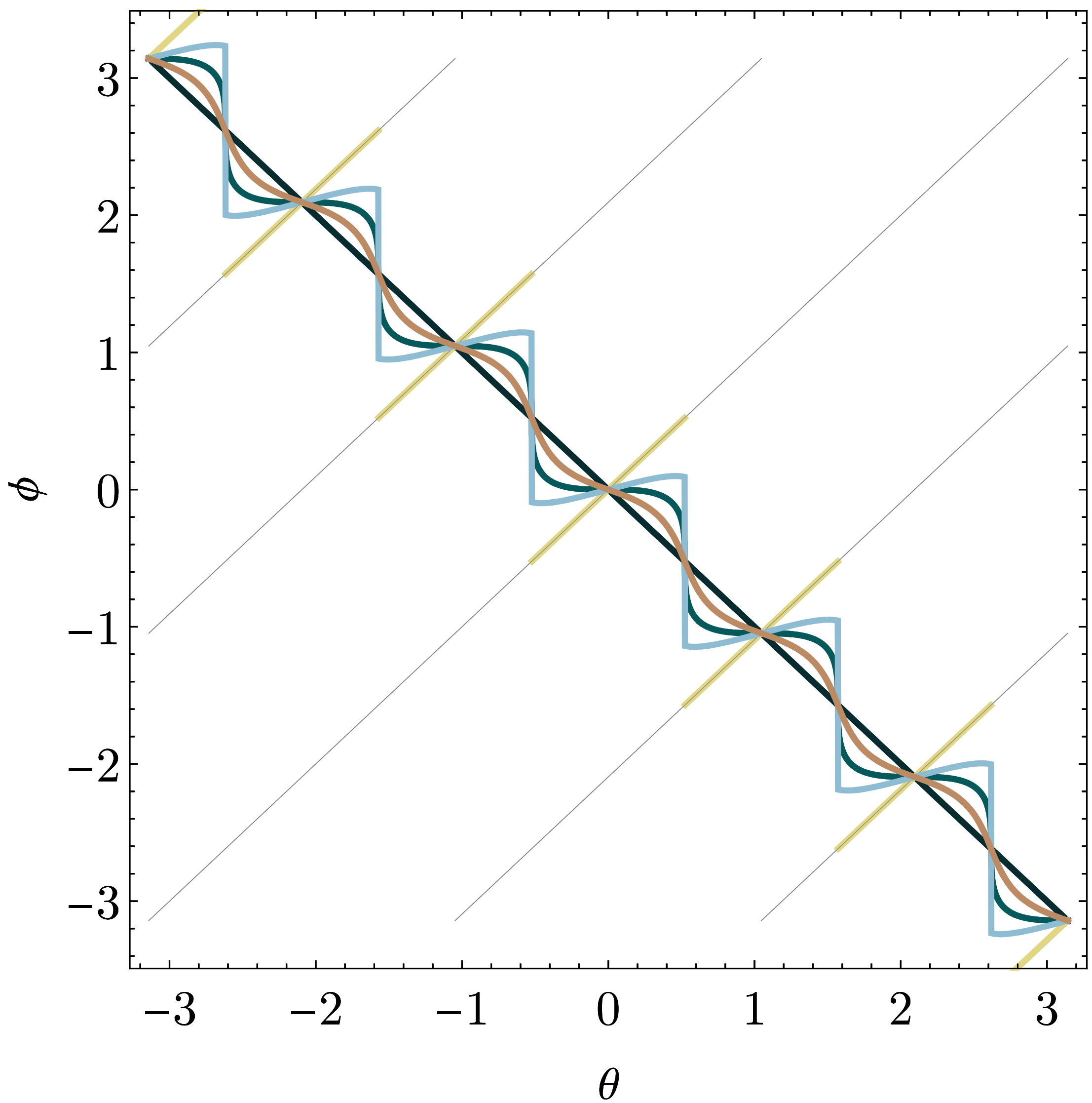

h>h_{crit}

Jumps at

$$\theta = \frac{\pi}{6} + \frac{\pi m}{3}$$

$$\theta = \frac{\pi}{6} + \frac{\pi m}{3}$$

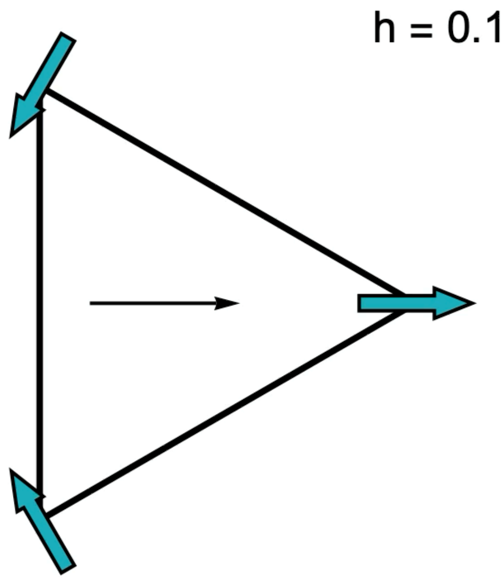

$h < h_c$

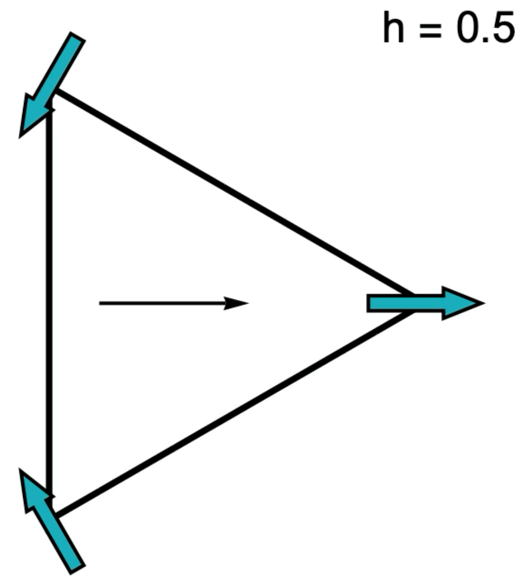

$h < h_c$

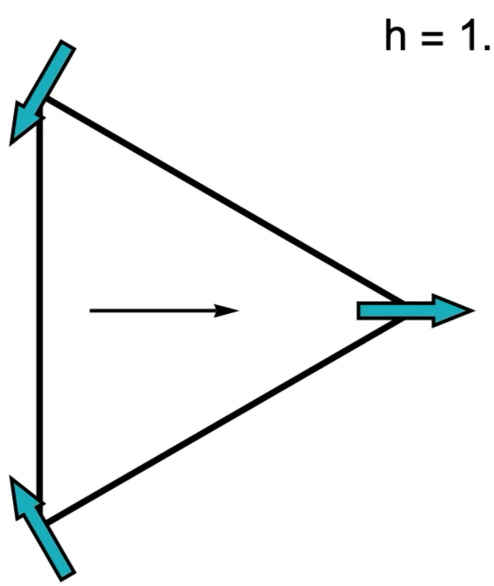

$h = h_c$

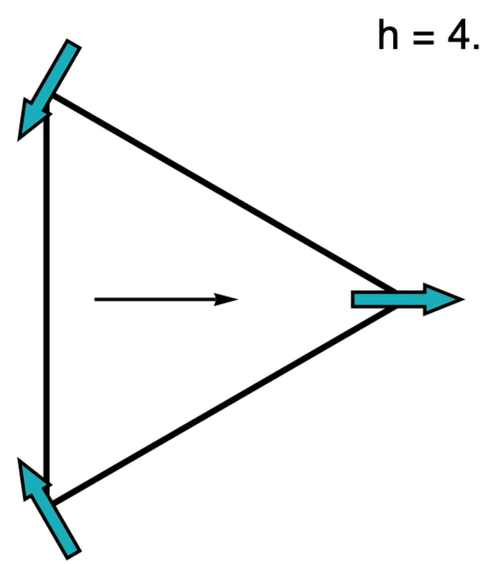

$h > h_c$

How do the jumps onset?

$$\psi = \phi + \theta, \qquad \theta = \pi/6 + \delta \qquad\qquad x = \sqrt{v/u}h^2$$

$$\frac{f}{uh} = -\cos\psi + x\cos 6\delta\cos 3\psi + x\sin 6\delta\sin 3\psi$$

$$= -\cos\psi + x\cos 3\psi \qquad (\delta = 0)$$

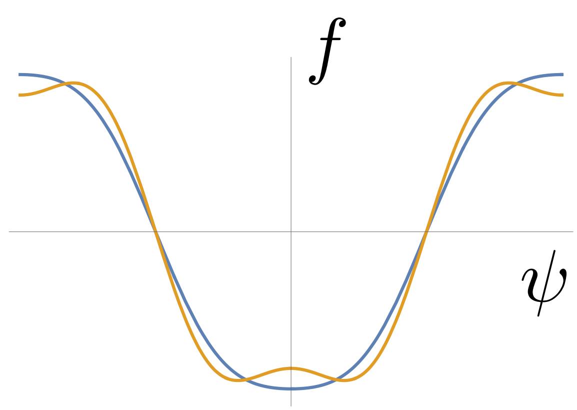

Ising transition
at x=1/9

δ acts as symmetry breaking field

Phase diagram

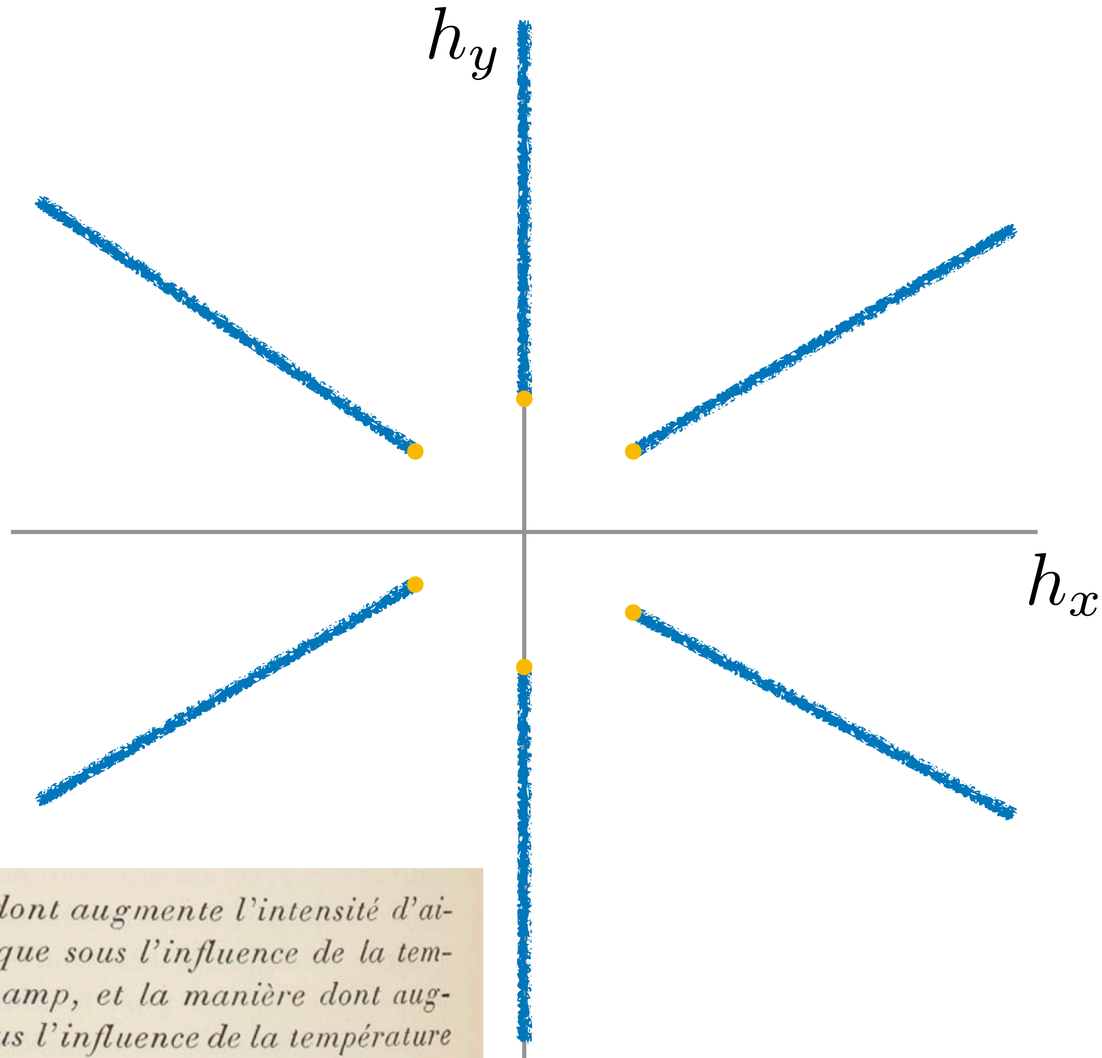

Analogie entre la manière dont augmente l'intensité d'aimantation d'un corps magnétique sous l'influence de la température et de l'intensité du champ, et la manière dont augmente la densité d'un fluide sous l'influence de la température et de la pression. — Il y a des analogies entre la fonction $f(\mathrm{I}, \mathrm{H}, \mathrm{T}) = 0$ relative à un corps magnétique et la fonction $f(\mathrm{D}, p, \mathrm{T}) = 0$ relative à un fluide. L'intensité d'aimantation I

Phase diagram

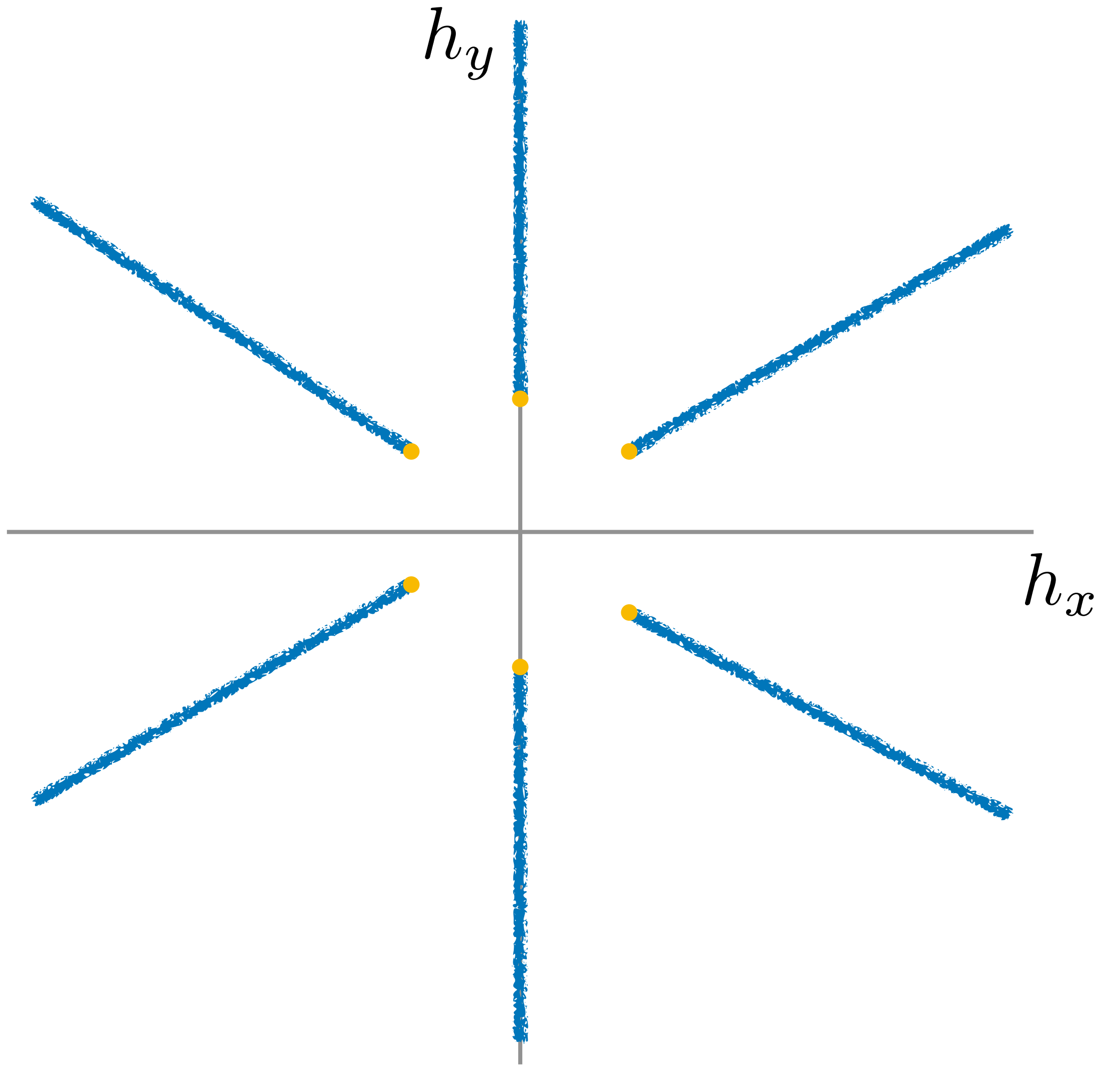

What symmetry is broken along the lines?

Mn_3Sn structure

$h \parallel \hat{y}$

glide

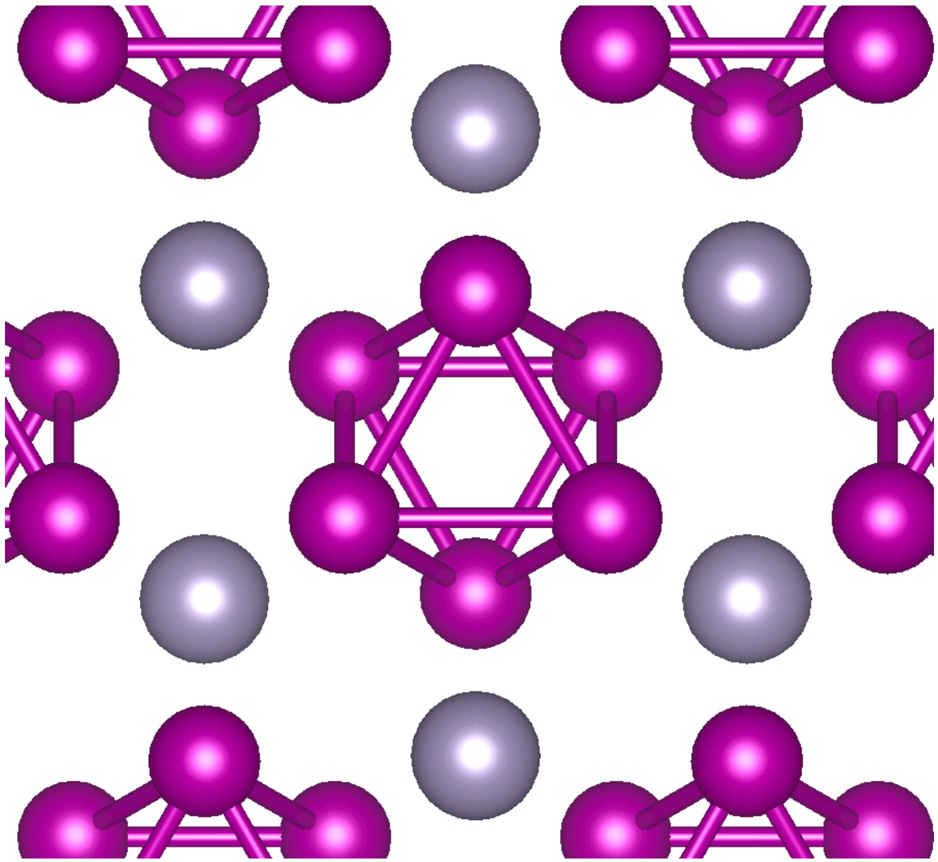

C_2

$h \parallel \hat{x}$

Torque

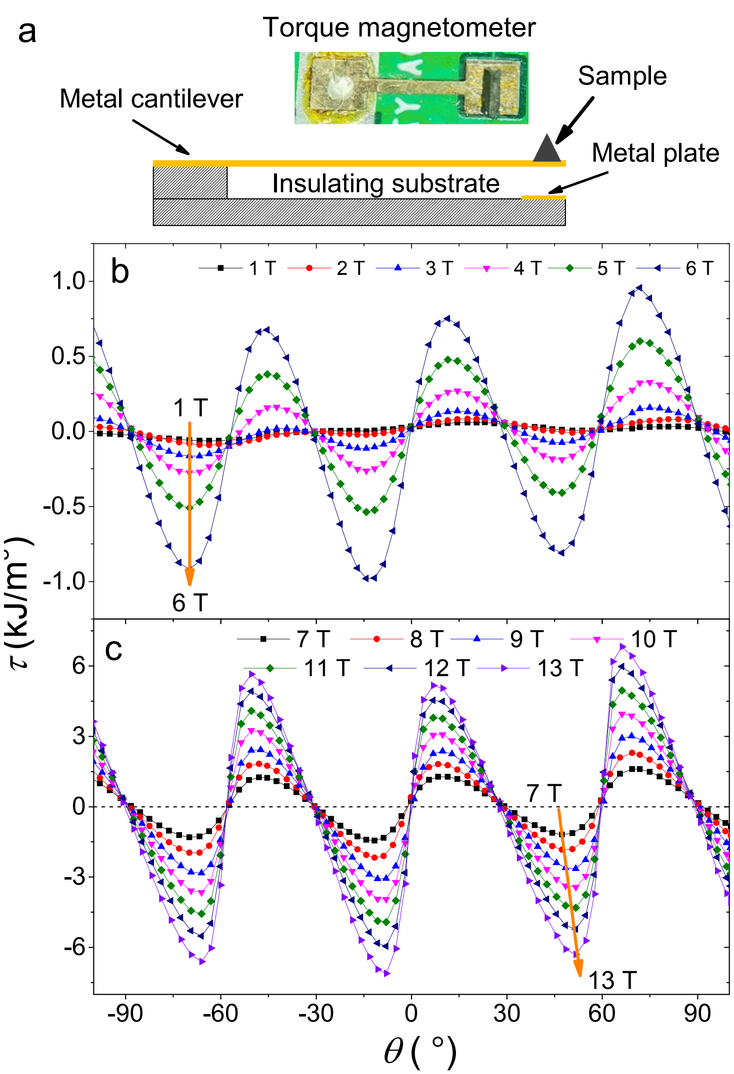

$$\tau = \frac{df}{d\theta}$$

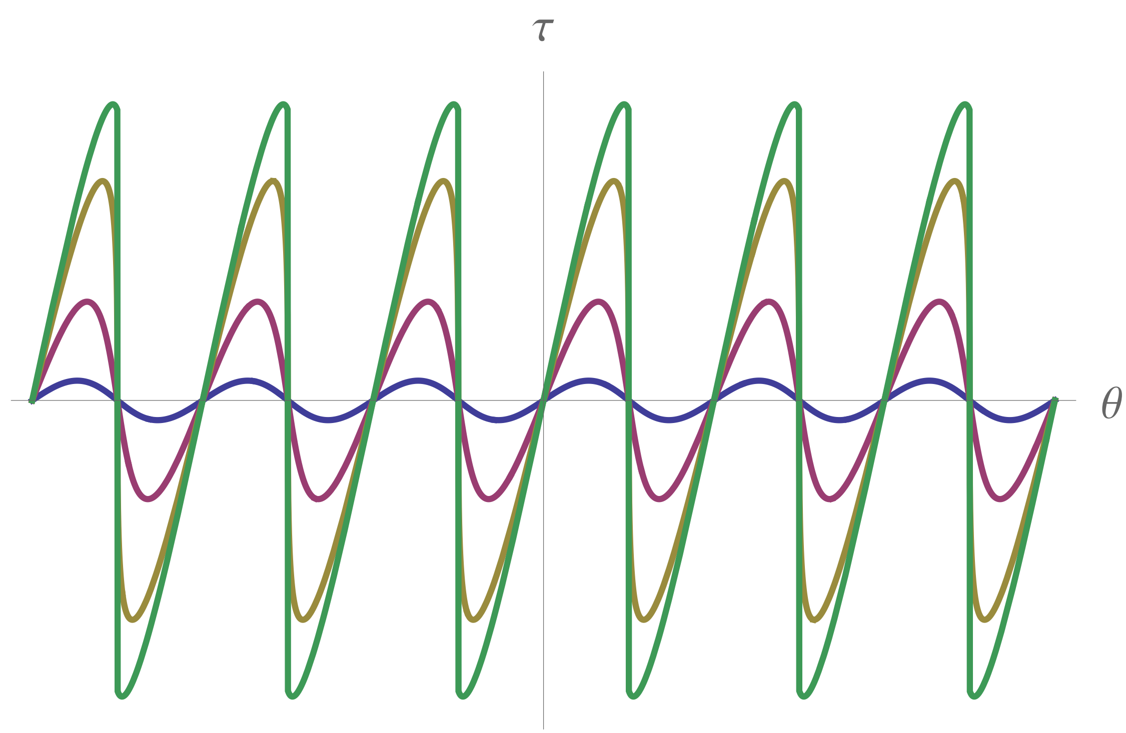

Discontinuities for h>h_c

Estimate

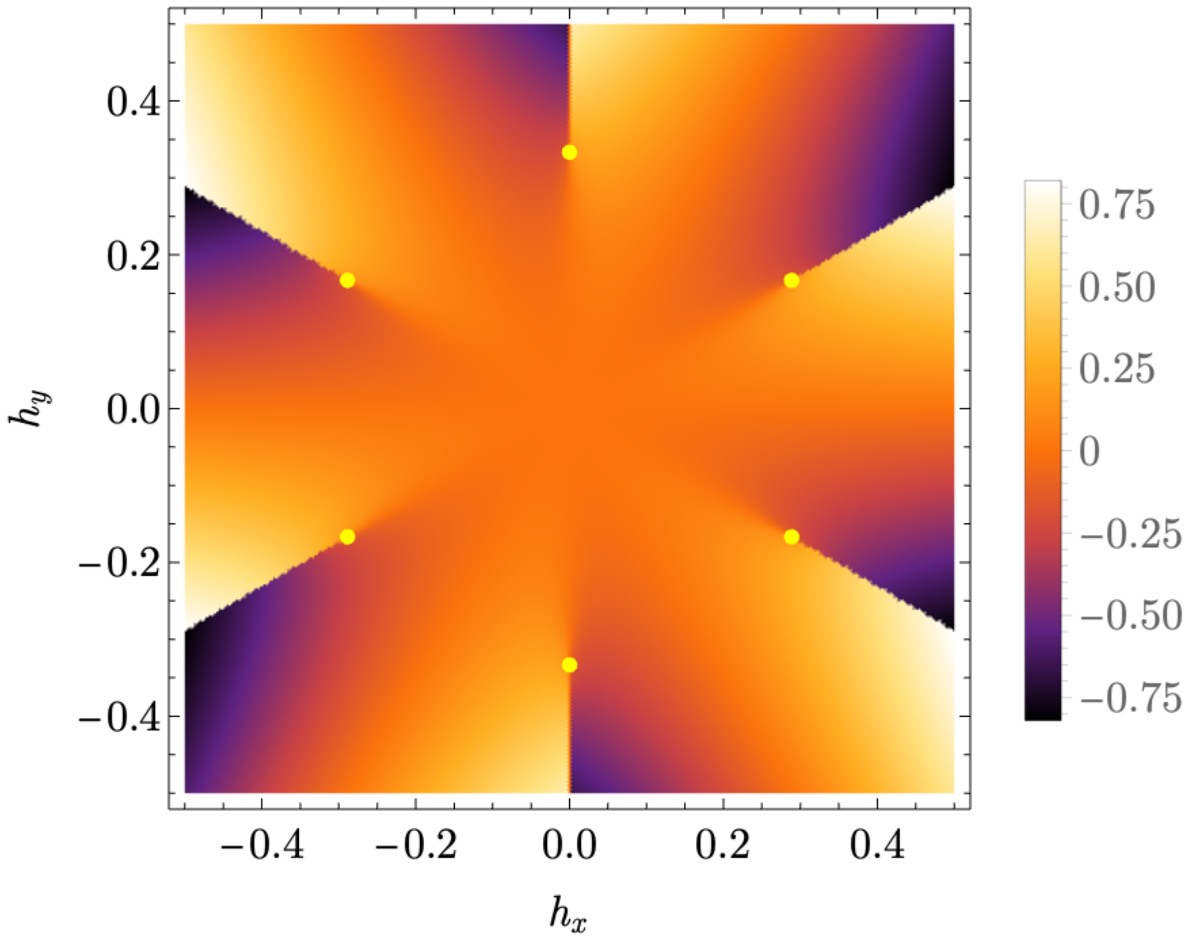

Classical, T=0

$$H_c = \frac{J + \sqrt{3}D}{g\mu_B}\sqrt{\frac{K}{D}}$$

$$\approx 20\text{T}$$

Estimate

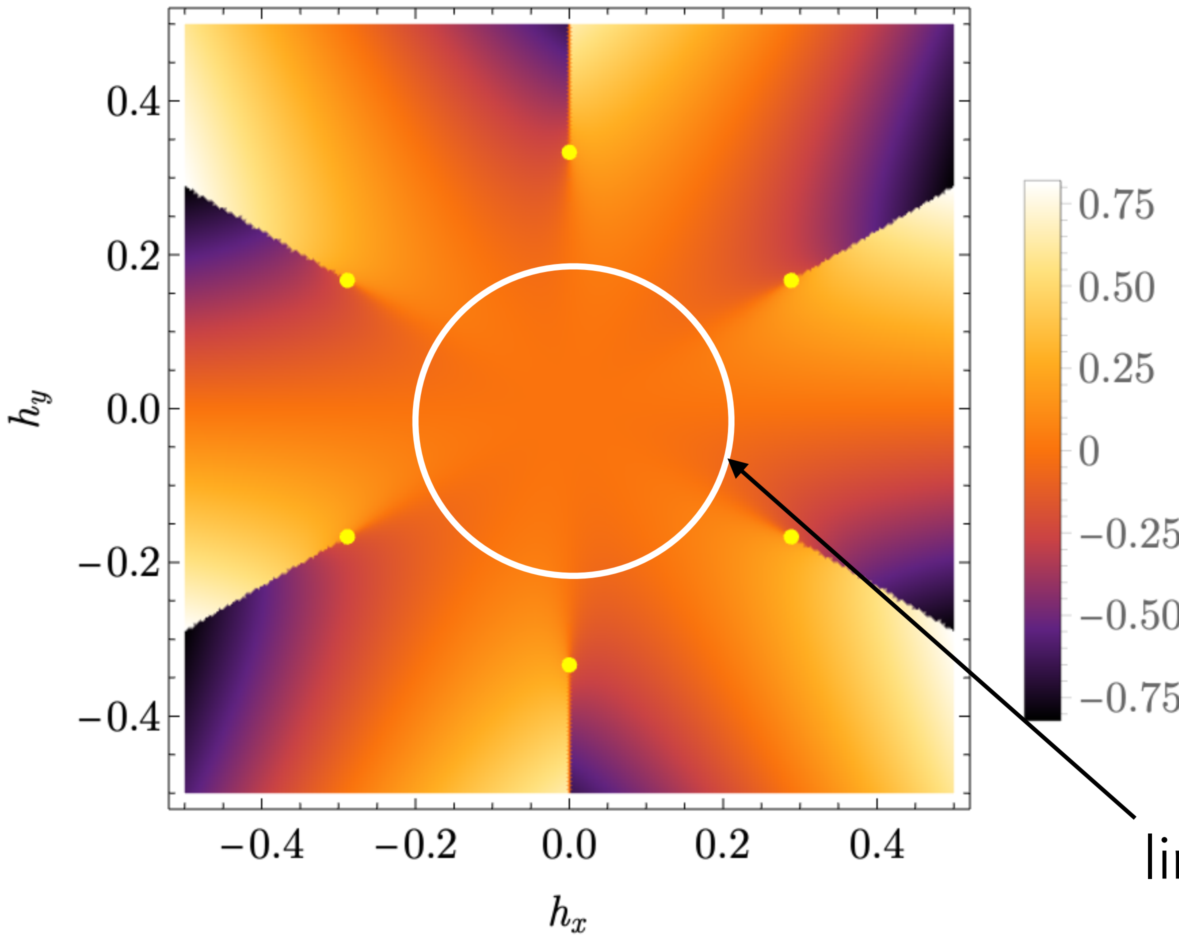

limit of current experiments

Classical, T=0

$$H_c = \frac{J + \sqrt{3}D}{g\mu_B}\sqrt{\frac{K}{D}}$$

$$\approx 20\mathrm{T}$$

Hope to observe these transitions in future experiments c.f.

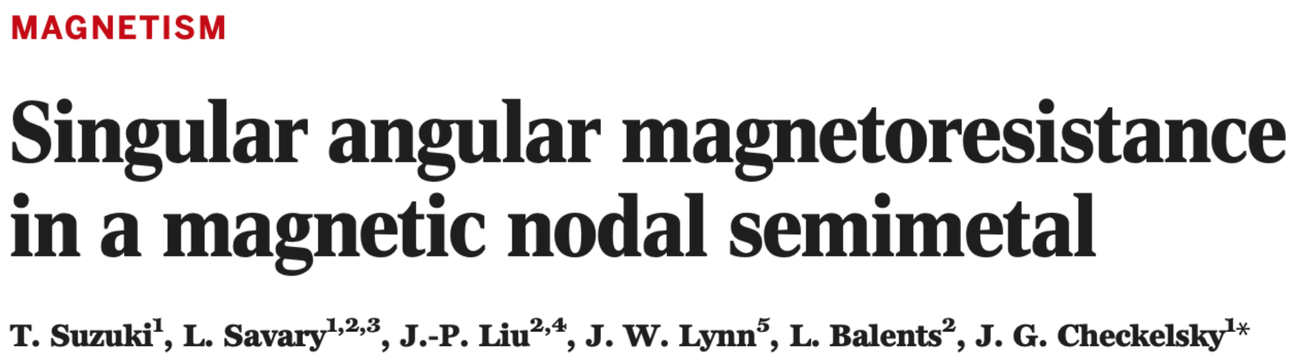
MAGNETISM

Singular angular magnetoresistance in a magnetic nodal semimetal

T. Suzuki[1], L. Savary[1,2,3], J.-P. Liu[2,4], J. W. Lynn[5], L. Balents[2], J. G. Checkelsky[1]*

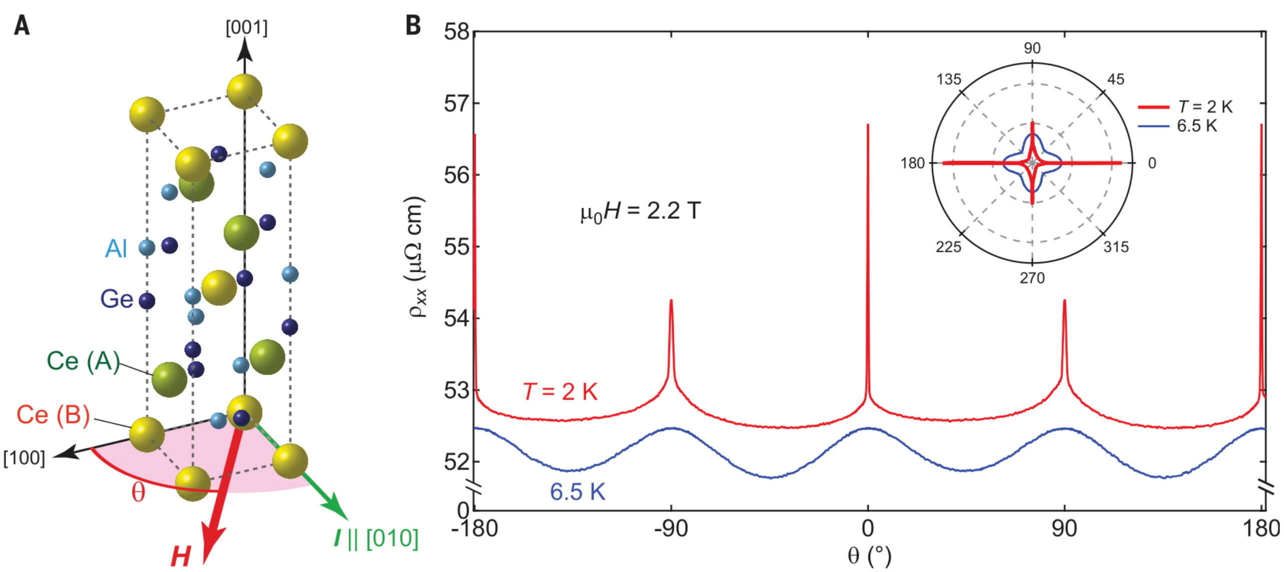

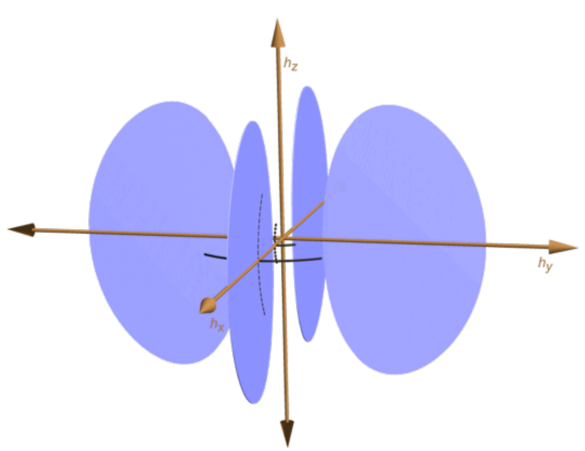

Would be interesting to search for transport signatures in Mn_3Sn

Strain control

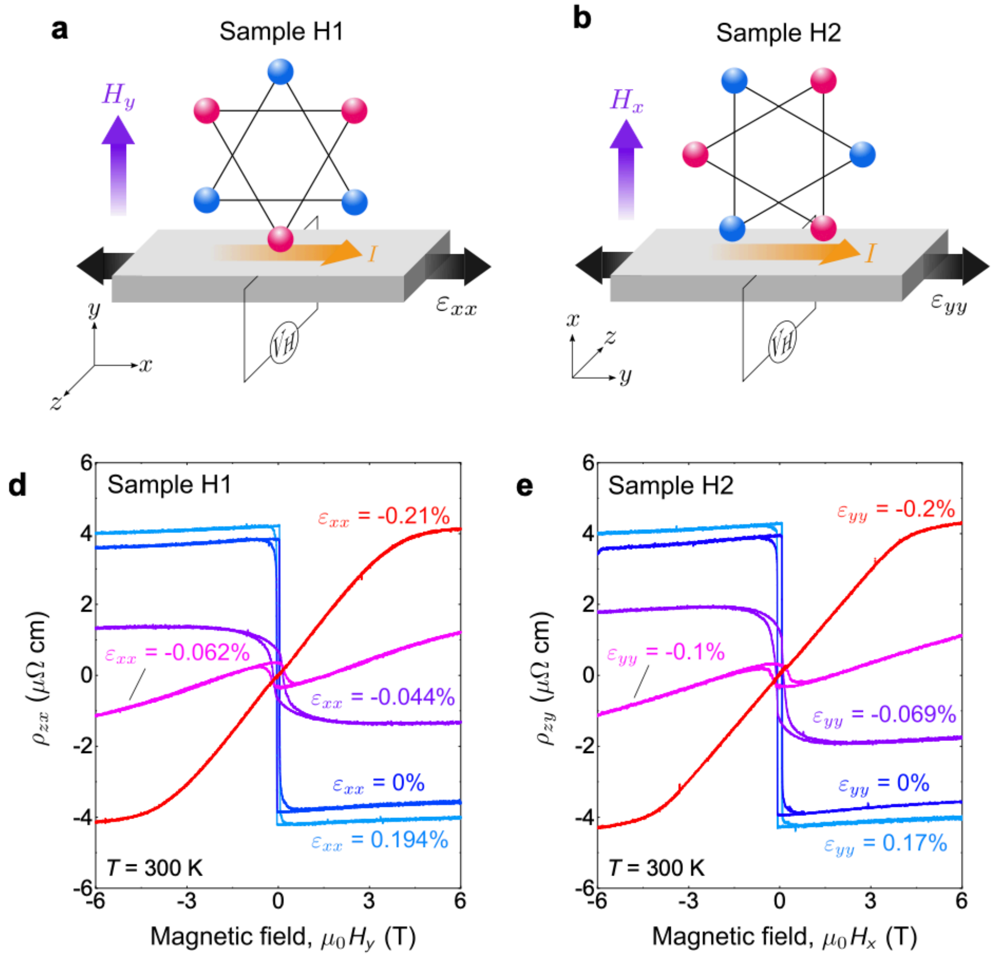

Strain also twists spins, allowing separate control of magnetization and Berry curvature

Ikhlas *et al*, arXiv:2206.00793 (2022)

Outline

- Twisting spins in Mn_3Sn with a magnetic field
  - Multiple energy scales enable control of anomalous Hall effect

Kamran Behnia
ESPCI

Zengwei Zhu
Wuhan

Xiaokang Li
Wuhan

- Twisting layers of spins in 2d materials
  - Twists control new spin textures

Kasra Hejazi
Caltech

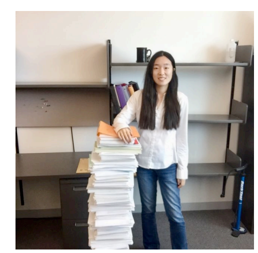

Zhu-Xi Luo
UCSB

2d VdW magnets

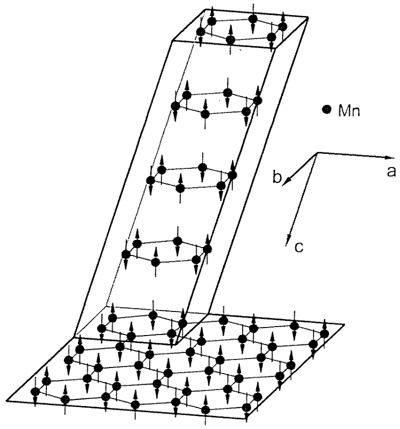

$MnPS_3$, $FePS_3$, $NiPS_3$, $CoPS_3$, $CrSiTe_3$...

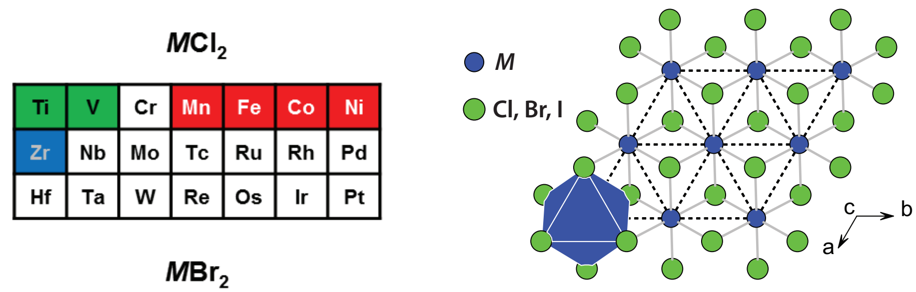

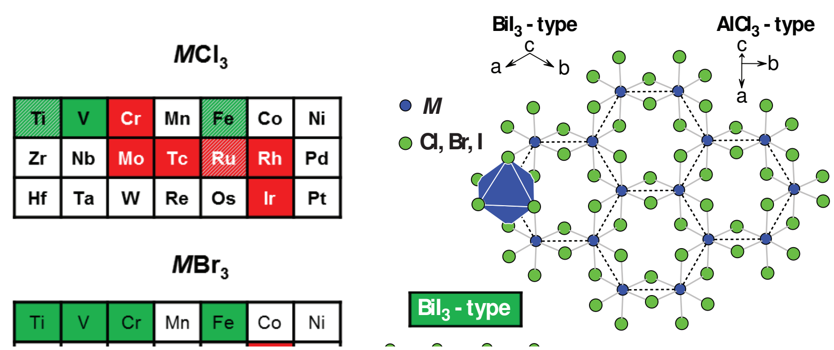

CrI_3, $RuCl_3$,…

CrI_3

B. Huang *et al*, 2017

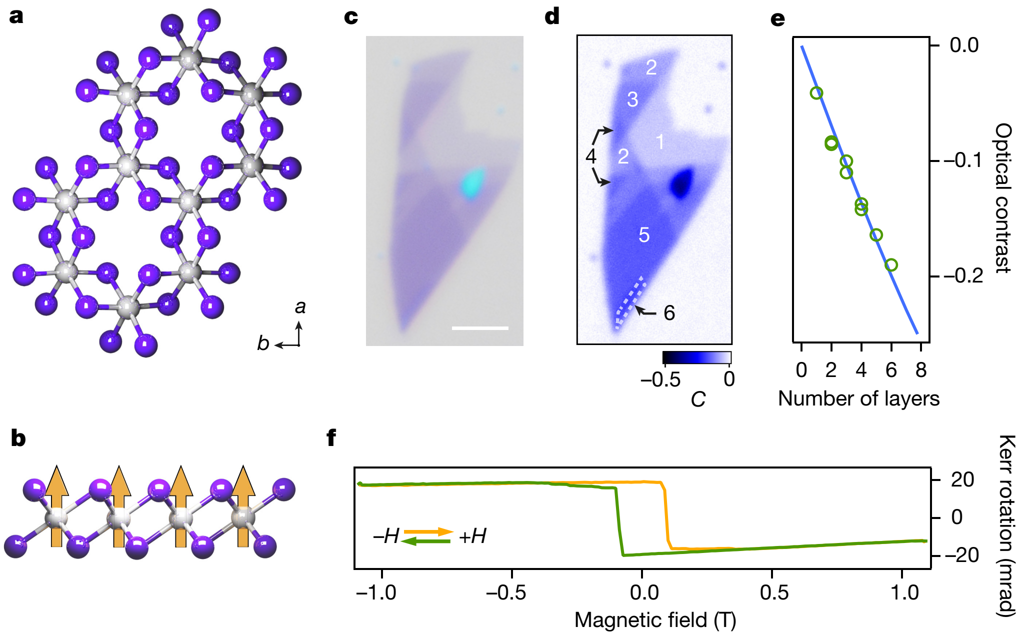

Ferromagnetic 2d honeycomb layers

Optical measurement of magnetization

1L

2L

3L

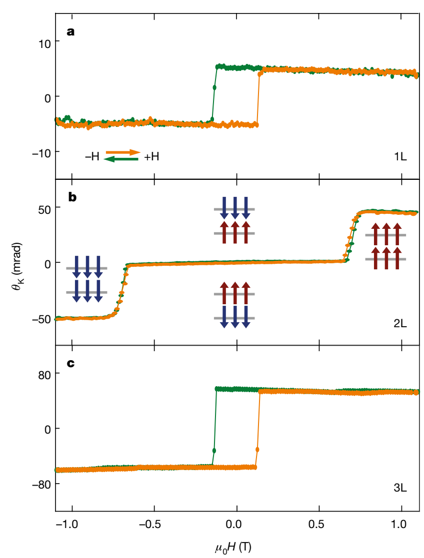

Still ferromagnetic in single layer

Surprise: bilayer is anti-ferromagnetic

$MnPS_3$

G. Long *et al*, 2020

antiferromagnetic
honeycomb

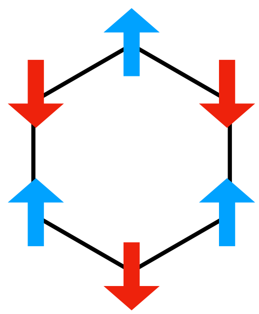

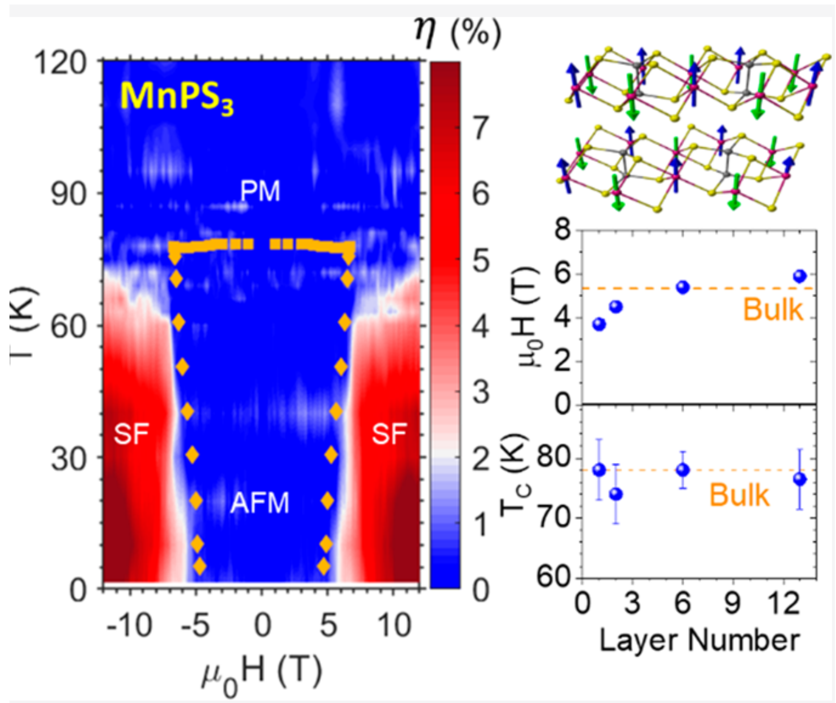

order persists to single layer

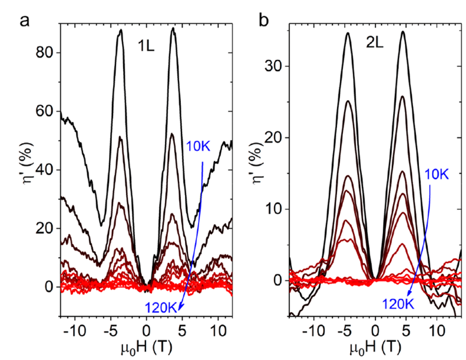

tunneling MR

MnPS$_3$

Direct Imaging of Antiferromagnetic Domains and Anomalous Layer-Dependent Mirror Symmetry Breaking in Atomically Thin MnPS$_3$

Zhuoliang Ni,[1] Huiqin Zhang,[2] David A. Hopper,[2,1] Amanda V. Haglund,[3] Nan Huang,[3] Deep Jariwala,[2] Lee C. Bassett,[2] David G. Mandrus,[3,4] Eugene J. Mele,[1] Charles L. Kane,[1] and Liang Wu[1,*]

PHYSICAL REVIEW LETTERS **127**, 187201 (2021)

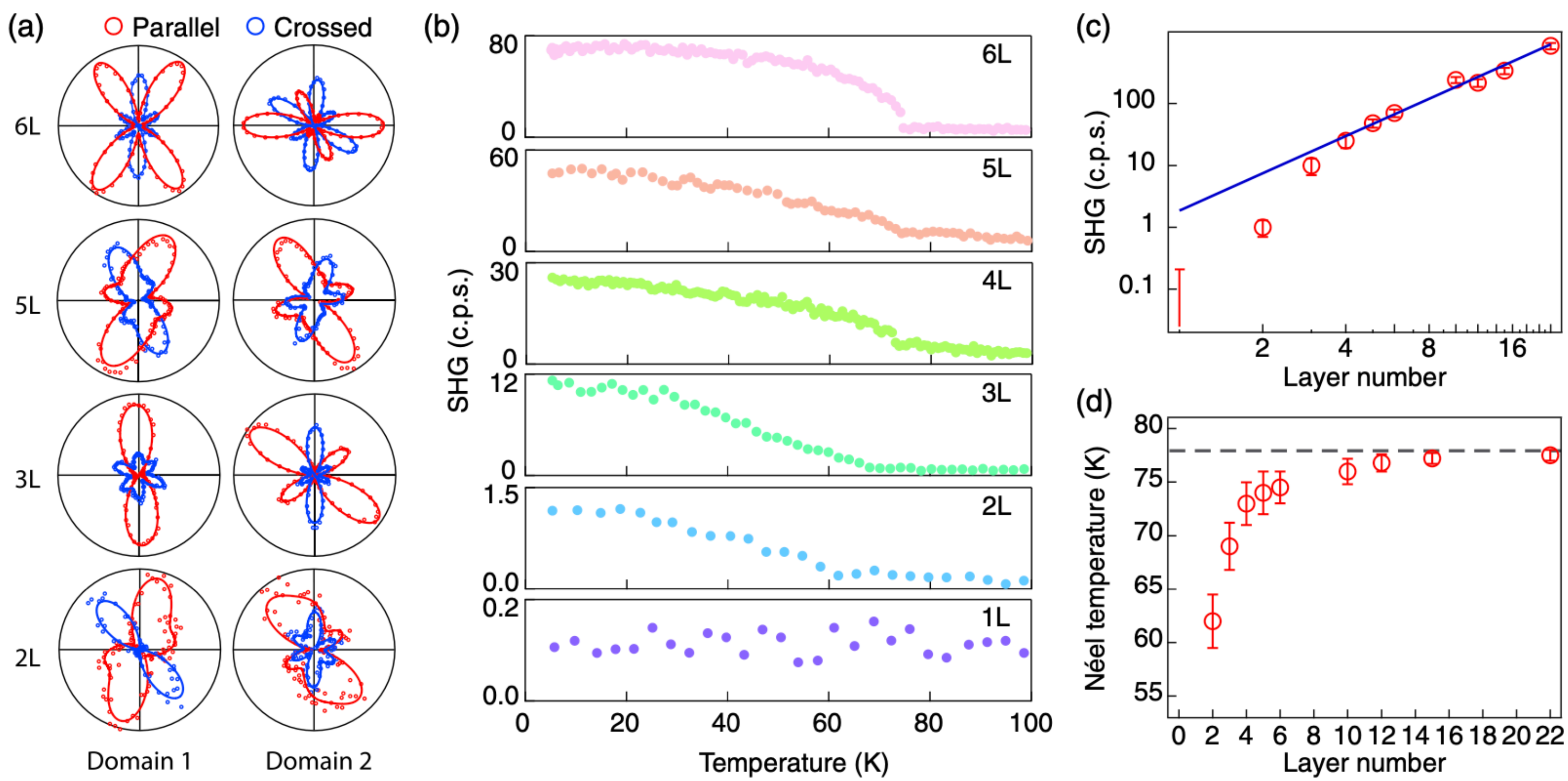

Twisting and moiré

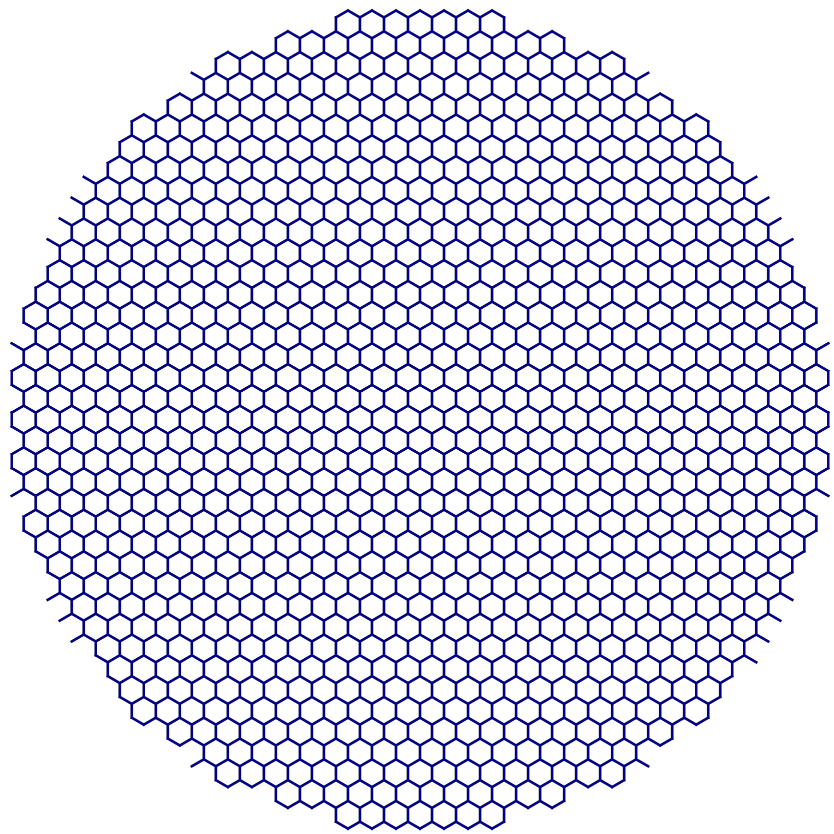

Moiré

mohair

Le retour de la moire

Le grand retour de la moire chez vous

La moire : Un tissu d'exception pour des murs, des rideaux et des meubles originaux

Moiré pattern

6°

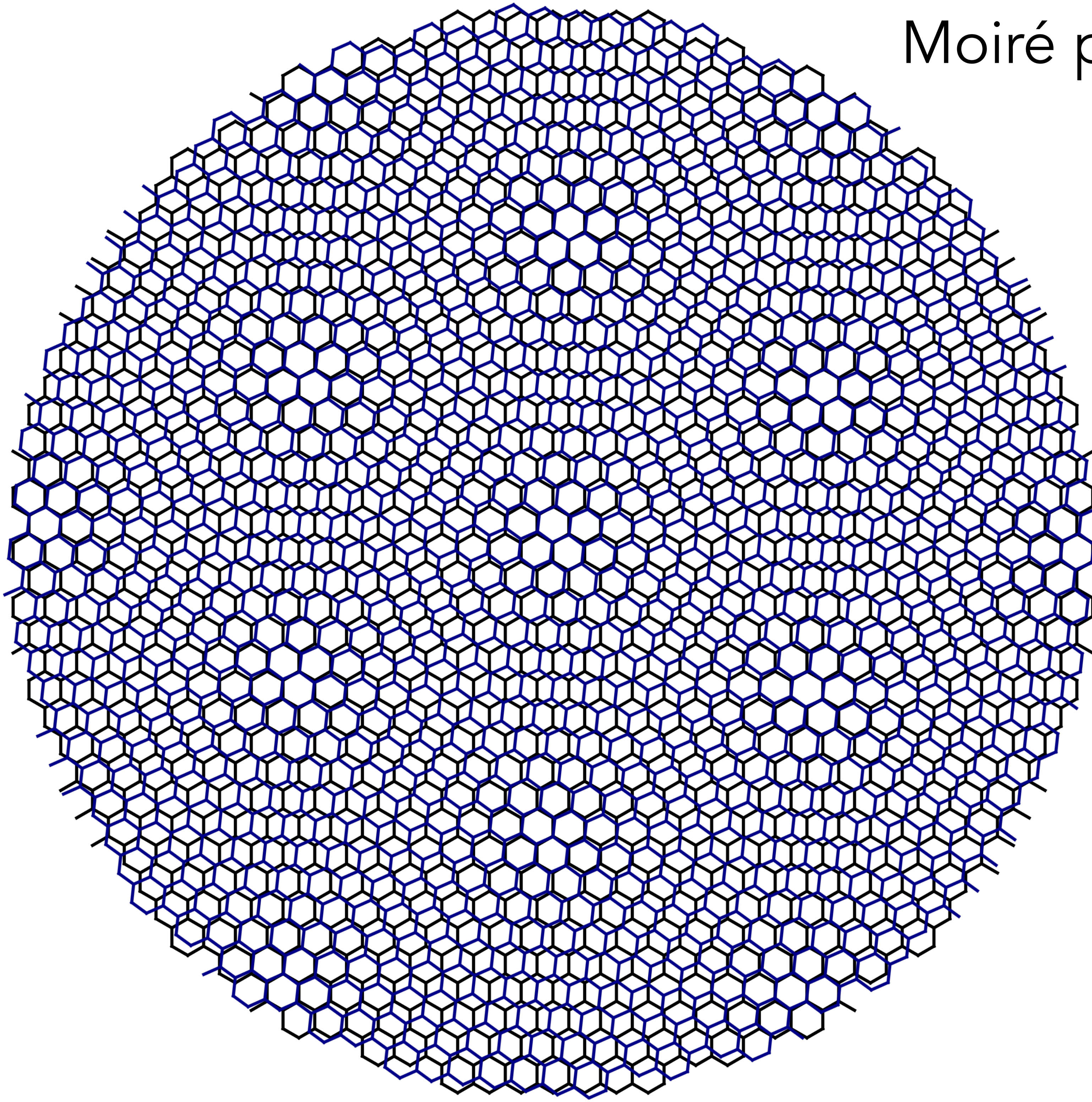

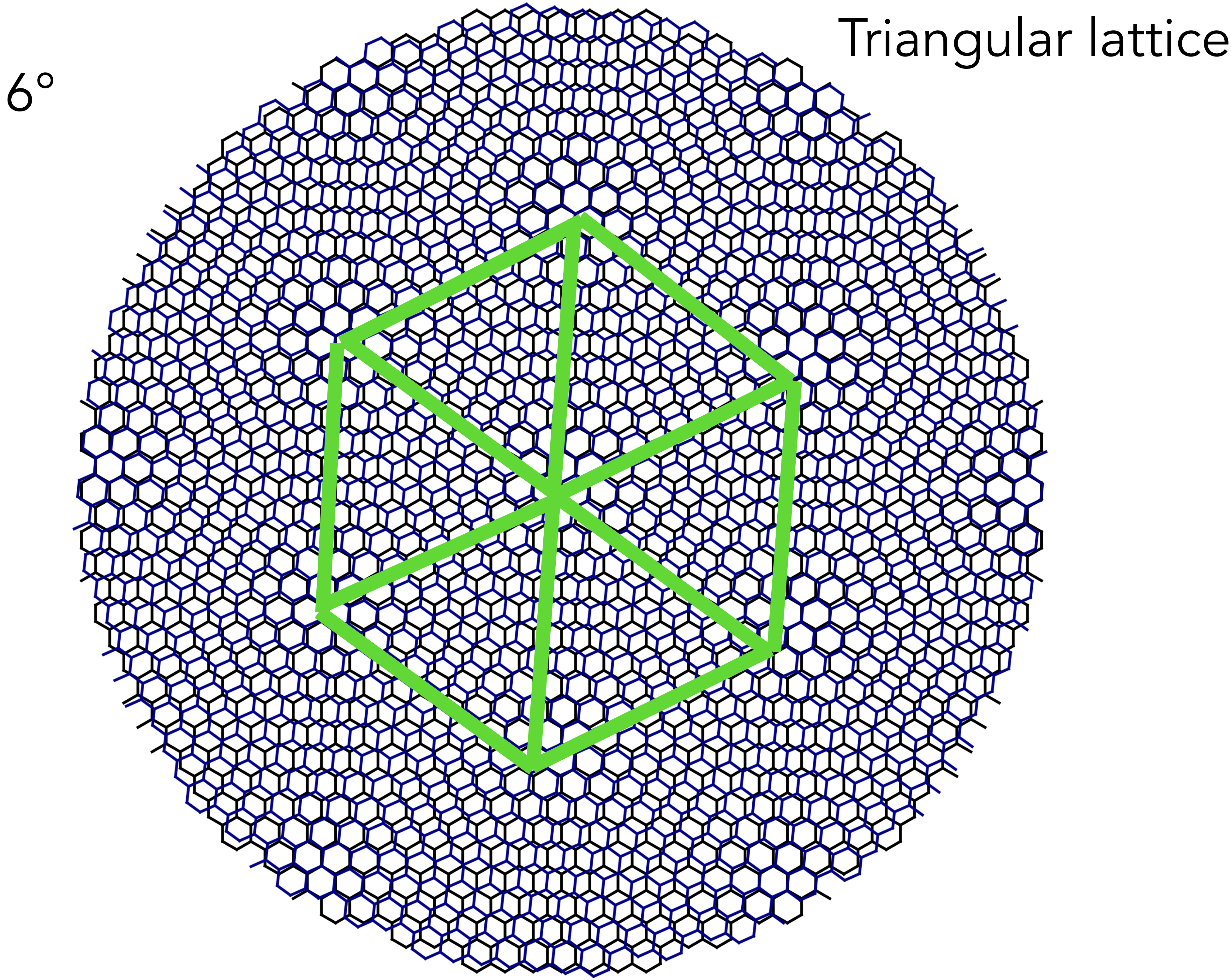
6°
Triangular lattice

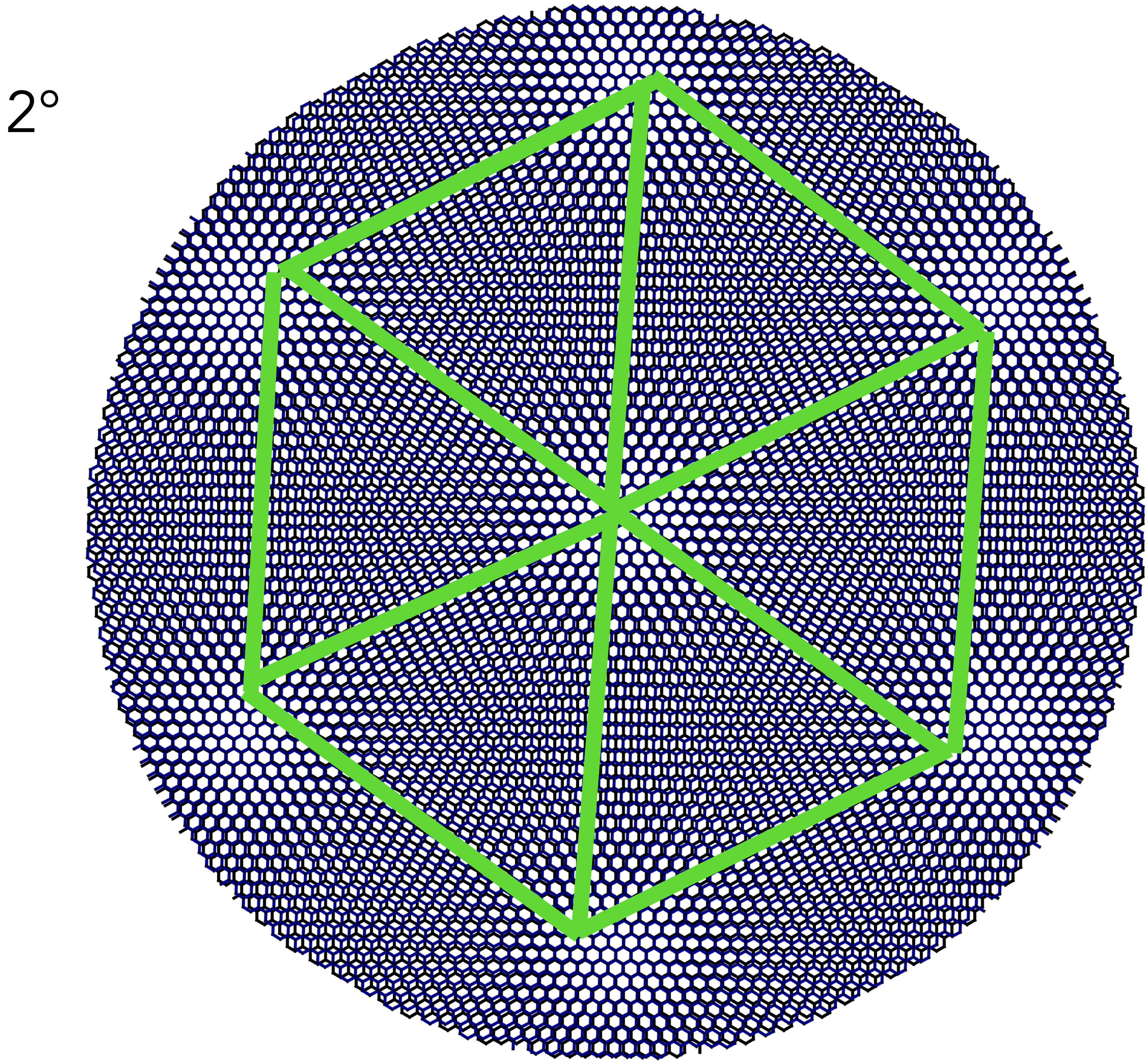
2°

1°

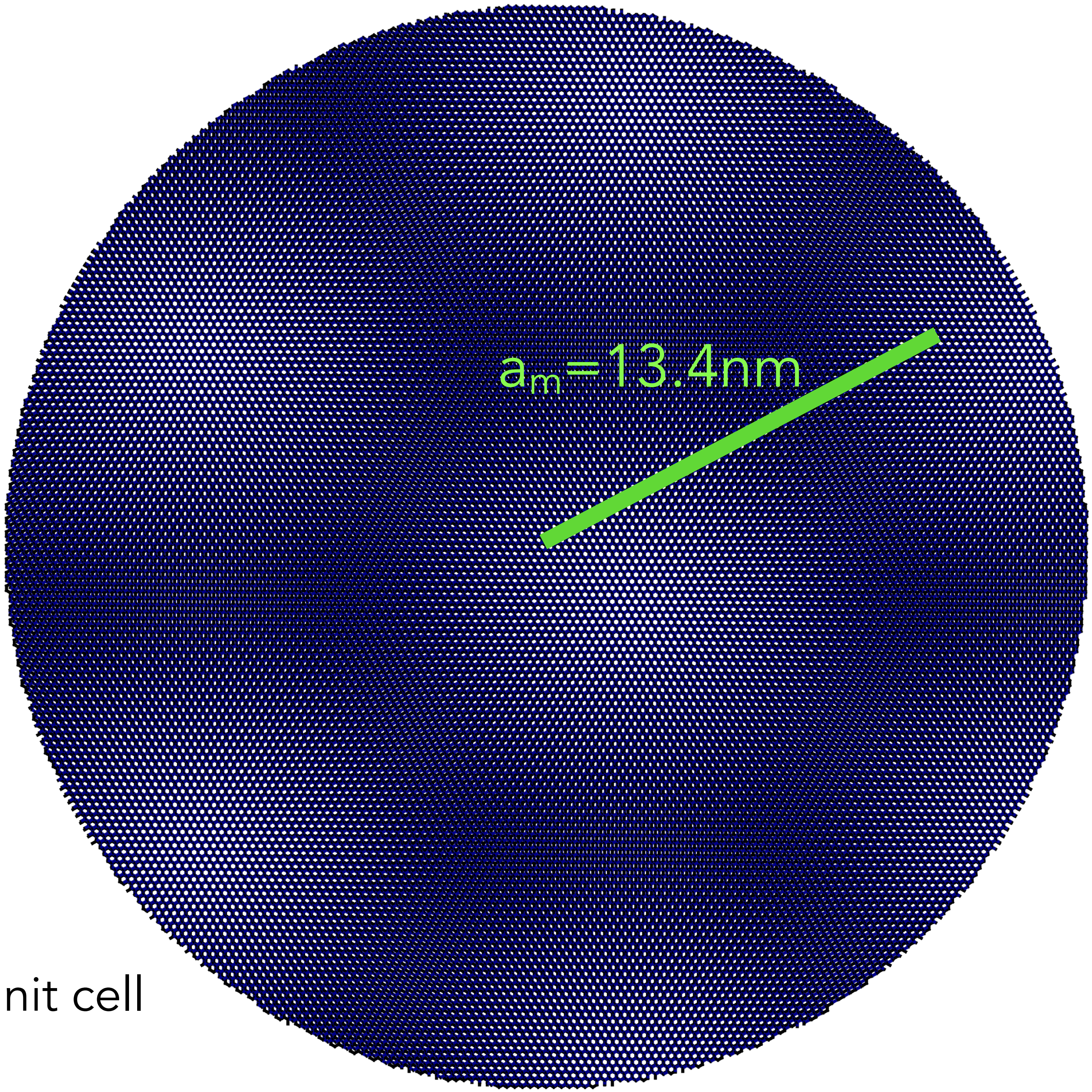

huge unit cell

6°

Twisted AF

Kasra Hejazi

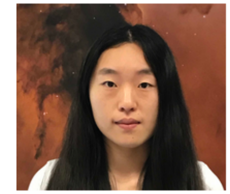

Zhu-Xi Luo

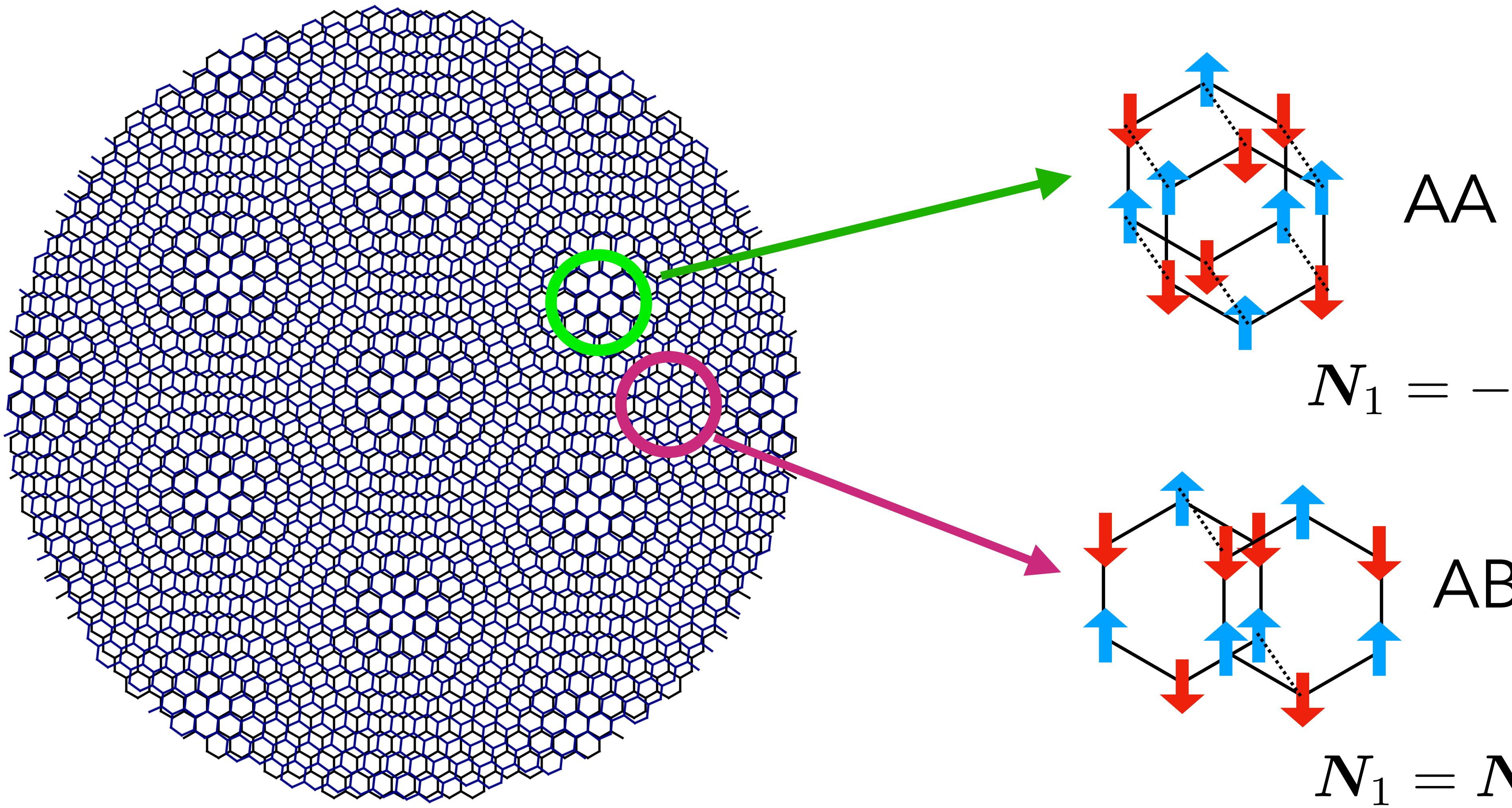

$$\boldsymbol{N}_1 = -\boldsymbol{N}_2$$

$$\boldsymbol{N}_1 = \boldsymbol{N}_2$$

Frustration: Neél vectors must rotate

Continuum model(s)

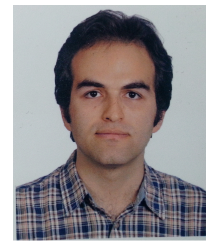

Kasra Hejazi

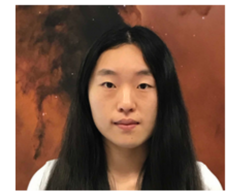

Zhu-Xi Luo

- Basic assumptions:
  - Inter-layer coupling weak J’ << J
  - Rotation angle is small (can also treat general strains)
- Example: $MnPS_3$: excellent Heisenberg AF

$$\mathcal{L} = \sum_l \frac{\rho}{2v^2} \left(\partial_t \boldsymbol{N}_l\right)^2 - \mathcal{H}_{\rm cl}$$

$$\mathcal{H}_{\rm cl} = \sum_l \left[\frac{\rho}{2} \left(\nabla \boldsymbol{N}_l\right)^2 - d\left(N_l^z\right)^2\right] - J'\Phi(\boldsymbol{x})\boldsymbol{N}_1 \cdot \boldsymbol{N}_2$$

$$\Phi(\boldsymbol{x}) = \sum_{a=1}^{3} \cos(\boldsymbol{q}_a \cdot \boldsymbol{x})$$

Can predict spin textures, magnon subbands, etc.

Twisted AF

$$\mathcal{H}_{\rm cl} = \sum_l \left[\frac{\rho}{2}(\nabla \boldsymbol{N}_l)^2 - d\,(N_l^z)^2\right] - J'\Phi(\boldsymbol{x})\boldsymbol{N}_1 \cdot \boldsymbol{N}_2$$

Dimensionless parameter $\alpha = \frac{2J'}{\rho q_m^2} \sim \frac{J'}{J\theta^2}$

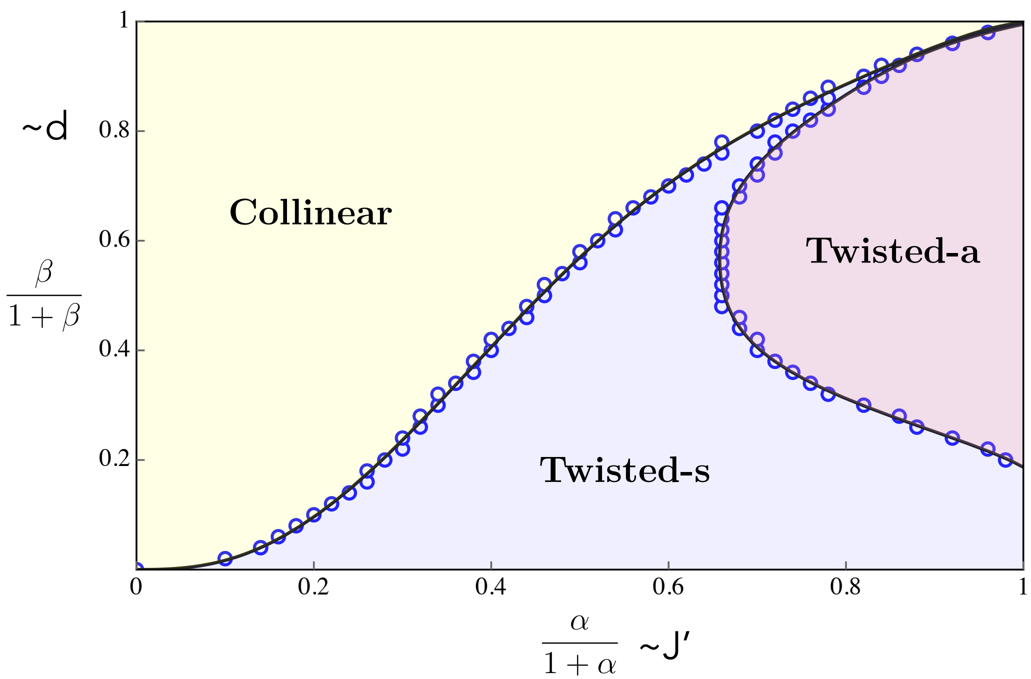

Coplanar spin textures

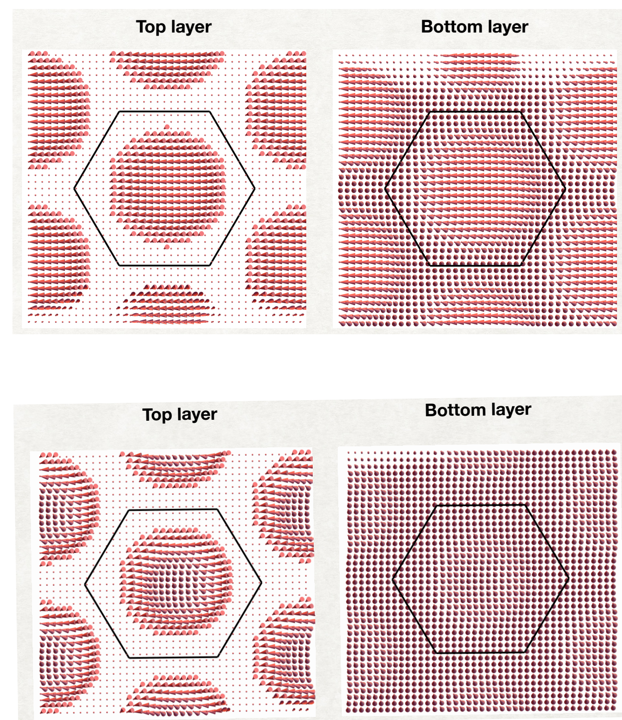

Transitions should be tunable by applied field

Zig-Zag antiferromagnets

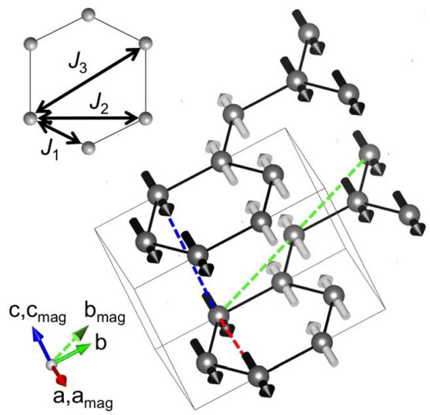

$$\mathcal{H}_{cl} = \sum_{a,l} \frac{\rho}{2} (\boldsymbol{\nabla} \boldsymbol{N}_{a,l})^2 - \frac{J'}{2} \sum_a \boldsymbol{N}_{a,1} \cdot \boldsymbol{N}_{a,2} \cos\left(\frac{\boldsymbol{q}_a \cdot \boldsymbol{x}}{2}\right)$$

3 distinct q_a domains

$NiPS_3$, $FePS_3$, $CoPS_3$, $RuCl_3$…

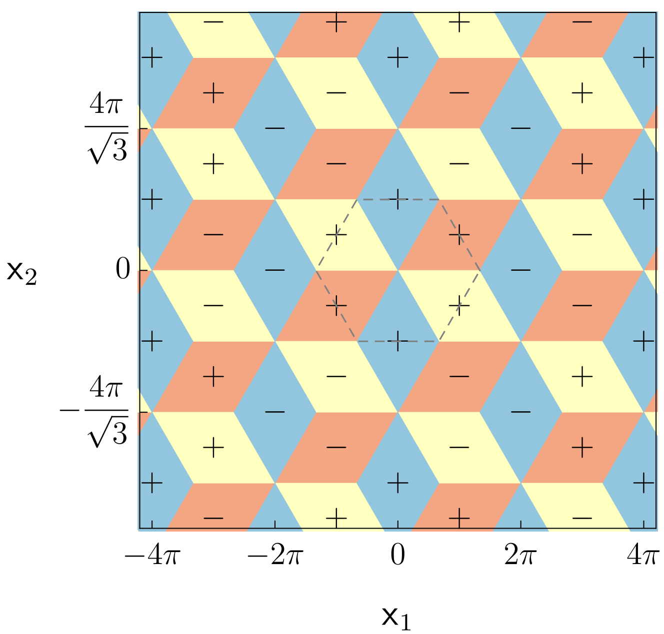

Strong-coupling domains have structure of "dice lattice"

CrI_3

Might not expect much from a *ferro*-magnet, but…

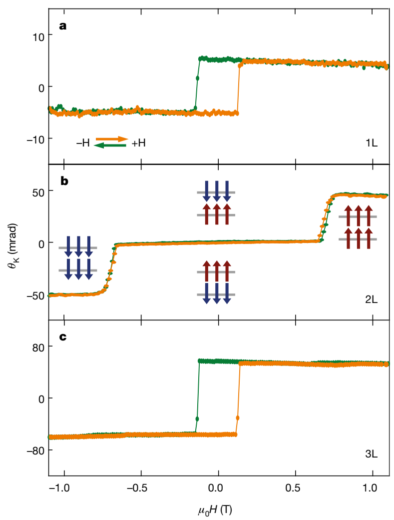

B. Huang *et al*, 2017

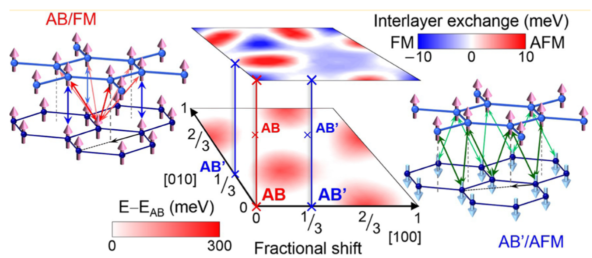

Sivadas *et al*, 2018

Sign-changing stacking-dependent interactions

$$\mathcal{H}_{\rm cl} = \sum_l \left[\frac{\rho}{2} \left(\nabla \boldsymbol{M}_l \right)^2 - d \left(M_l^z \right)^2 \right] - J' \tilde{\Phi}(\boldsymbol{x}) \boldsymbol{M}_1 \cdot \boldsymbol{M}_2$$

↑

from DFT theory

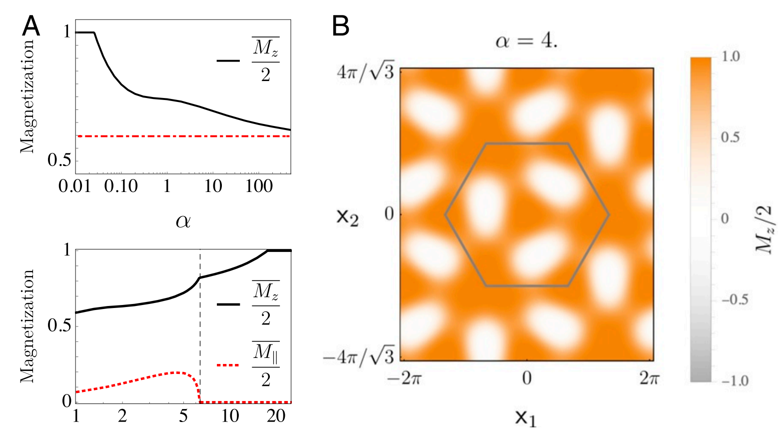

mixed

non-collinear

FM

CrI_3

nature nanotechnology
LETTERS
https://doi.org/10.1038/s41565-021-01014-y
Check for updates

Coexisting ferromagnetic–antiferromagnetic state in twisted bilayer CrI_3

Yang Xu[1,2], Ariana Ray[3], Yu-Tsun Shao[1], Shengwei Jiang[3], Kihong Lee[3], Daniel Weber[4], Joshua E. Goldberger[4], Kenji Watanabe[5], Takashi Taniguchi[6], David A. Muller[1,7], Kin Fai Mak[1,3,7] and Jie Shan[1,3,7]

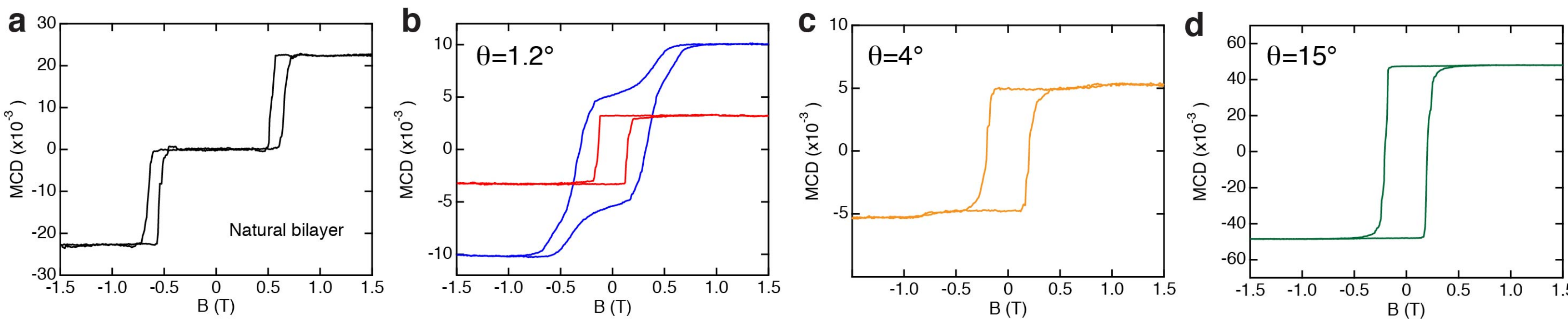

bilayer: AF

small twist: mixed

large twist: FM

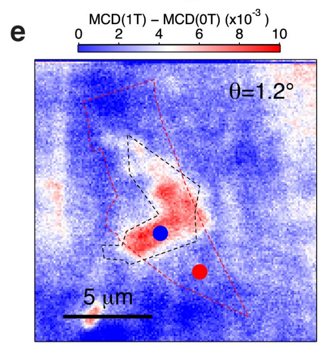

c.f.

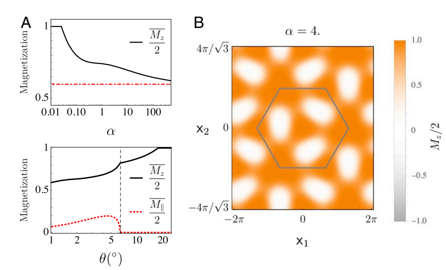

CrI_3

REPORT

MAGNETISM

Direct visualization of magnetic domains and moiré magnetism in twisted 2D magnets

Tiancheng Song[1]†, Qi-Chao Sun[2]†, Eric Anderson[1]†, Chong Wang[3], Jimin Qian[4], Takashi Taniguchi[5], Kenji Watanabe[6], Michael A. McGuire[7], Rainer Stöhr[2,8], Di Xiao[3], Ting Cao[4], Jörg Wrachtrup[2,9]*, Xiaodong Xu[1,4]*

Scanning NV magnetometry

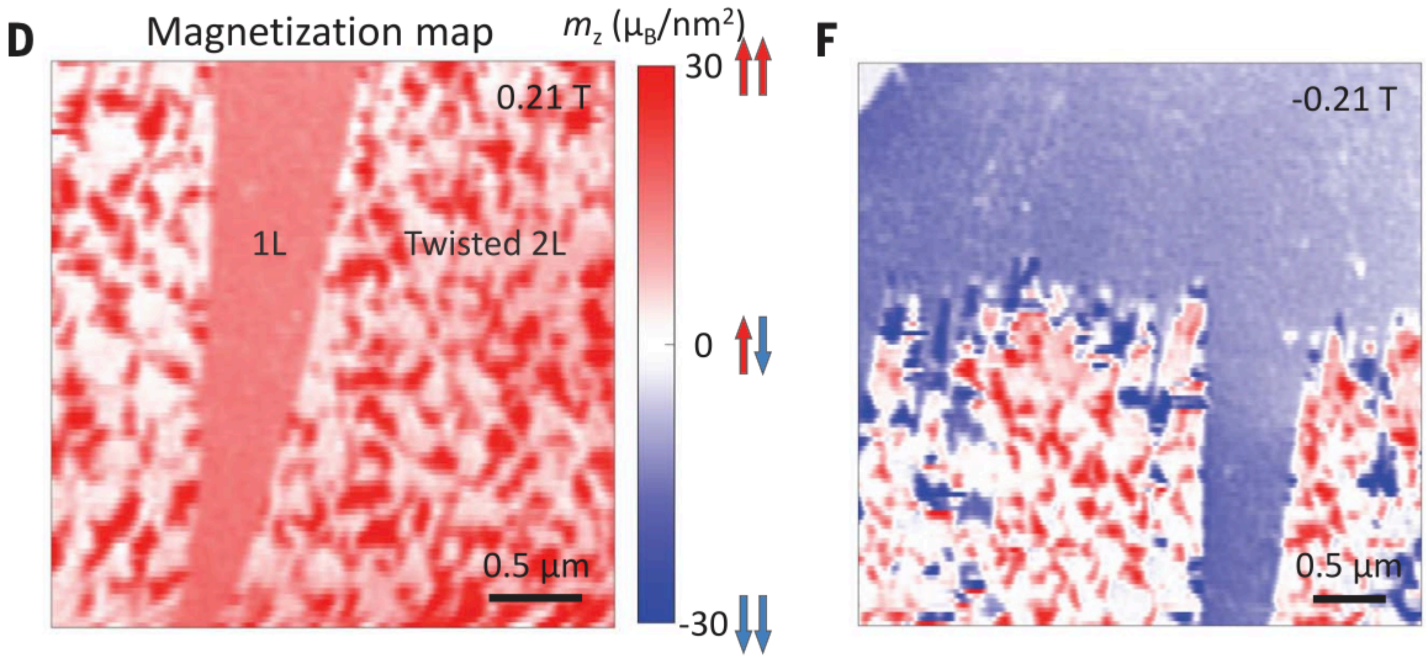

(twist disorder is evident)

Merci

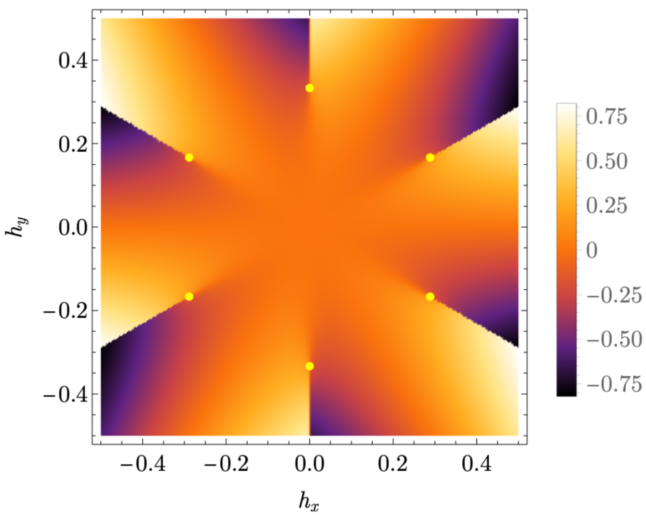

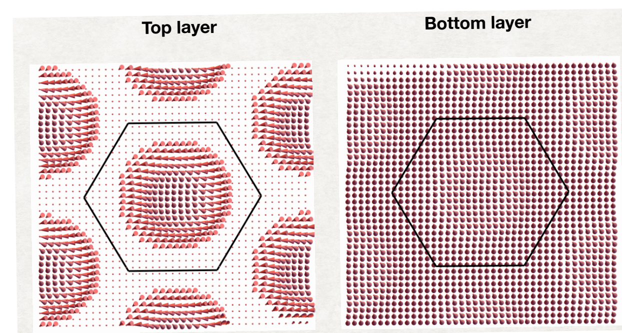

Office of Basic Energy Sciences
Serving the Present, Shaping the Future
NSF
Simons Collaboration on Ultra-Quantum Matter
UC SANTA BARBARA Quantum Foundry
DMR-1906325
CIFAR